

1
2
3 **Analysis of New Particle Formation (NPF) Events at**
4 **Nearby Rural, Urban Background and**
5 **Urban Roadside Sites**
6
7

8 **Dimitrios Bousiotis¹, Manuel Dall'Osto², David C.S. Beddows¹,**
9 **Francis D. Pope¹ and Roy M. Harrison^{1a*}**

10
11 **¹ School of Geography, Earth & Environmental Sciences and**
12 **National Centre for Atmospheric Science**
13 **University of Birmingham, Edgbaston, Birmingham**
14 **B15 2TT, United Kingdom**
15

16 **² Institute of Marine Sciences, CSIC**
17 **Passeig Marítim de la Barceloneta, 37-49. E-08003**
18 **Barcelona, Spain**
19
20

21
22 ^aAlso at: Department of Environmental Sciences / Center of Excellence in Environmental Studies, King Abdulaziz
23 University, PO Box 80203, Jeddah, 21589, Saudi Arabia
24

25 * To whom correspondence should be addressed.
26 Tele: +44 121 414 3494; Fax: +44 121 414 3709; Email: r.m.harrison@bham.ac.uk
27
28

29 ABSTRACT

30 New Particle Formation (NPF) events have different patterns of development depending on the
31 conditions of the area in which they occur. In this study, particle size distributions in the range of 16.6
32 – 604 nm (seven years of data) were analysed and NPF events occurring at three sites of differing
33 characteristics (rural Harwell (HAR), urban background North Kensington (NK), urban roadside
34 Marylebone Road (MR), London, UK) were extracted and studied. The different atmospheric
35 conditions in each study area not only have an effect on the frequency of the events, but also affect
36 their development. The frequency of NPF events is similar at the rural and urban background locations
37 (about 7% of days), with a high proportion of events occurring at both sites on the same day (45%).
38 The frequency of NPF events at the urban roadside site is slightly less (6% of days), and higher
39 particle growth rates (average 5.5 nm h⁻¹ at MR compared to 3.4 nm h⁻¹ and 4.2 nm h⁻¹ at HAR and
40 NK respectively) must result from rapid gas to particle conversion of traffic-generated pollutants. A
41 general pattern is found in which the condensation sink increases with the degree of pollution of the
42 site, but this is counteracted by increased particle growth rates at the more polluted location. A key
43 finding of this study is that the role of the urban environment leads to an increment of 20% in N₁₆₋
44 _{20nm} in the urban background compared to that of the rural area in NPF events occurring at both sites.
45 The relationship of the origin of incoming air masses is also considered and an association of regional
46 events with cleaner air masses is found. Due to lower availability of condensable species, NPF events
47 that are associated with cleaner atmospheric conditions have lower growth rates of the newly formed
48 particles. The decisive effect of the condensation sink in the development of NPF events and the

49 survivability of the newly formed particles is underlined, and influences the overall contribution of
50 NPF events to the number of ultrafine particles in an area. The other key factor identified by this
51 study is the important role that pollution, both from traffic and other sources in the urban environment
52 (such as heating or cooking), plays in new particle formation events.

53

54

1. INTRODUCTION

Ultrafine particles (particles with diameter smaller than 100 nm) typically make the greatest contribution in the total particle count, especially in urban environments (Németh et al., 2018), but a very small contribution to total volume and mass (Harrison et al., 2000). Research studies have indicated that ultrafine particles can cause pulmonary inflammation and may contribute to cardiovascular disease (Oberdörster, 2000) and have increased possibility to penetrate the brain and central nervous system (Politis et al., 2008) compared to fine and coarser particles. Since some studies report that toxicity per unit mass increases as particle size decreases (Penttinen et al., 2001; MacNee et al., 2003; Davidson et al., 2005); it is considered possible that particle number concentrations may be a better predictor of health effects than mass concentrations (Harrison et al., 2000; Atkinson et al., 2010; Kelly et al., 2012; Samoli et al., 2016). Additionally, NPF events have an impact on climate (Makkonen et al., 2012) either by increasing the number of cloud condensation nuclei (Spracklen et al., 2008; Merikanto et al., 2009; Dameto de España et al., 2017; Kalkavouras et al., 2017), or directly affecting the optical properties of the atmosphere (Seinfeld and Pandis, 2012).

The sources of ultrafine particles in urban areas can either be primary particles or emission sources from traffic (Shi et al., 1999; Harrison et al., 2000), airports (Masiol et al., 2017) and other combustion related processes (Keuken et al., 2015; Kecorius et al., 2016), or by new particle formation (NPF) from gaseous precursors. New particle formation as described by Kulmala et al. (2014), is the process of production of low-volatility vapours, clustering of these vapours, nucleation, activation of the

75 clusters with a second group of vapours and condensational growth to larger sizes. This process can
76 occur both locally or on a larger scale; in the latter case the events are characterized as regional.
77 Regional events have been found to take place in a scale of hundreds of kilometres (Németh and
78 Salma, 2014; Shen et al., 2018), without being affected by air mass advection (Salma et al., 2016).
79 NPF is one of the main contributors of particles in the atmosphere (Spracklen et al., 2010; Kulmala
80 et al., 2016; Rahman et al., 2017) and this relative contribution increases moving from a kerbside to
81 a rural area (Ma and Birmili, 2015). While NPF events in rural and remote areas have been widely
82 studied for many years (O'Dowd et al., 2002; Dal Maso et al., 2005; Ehn et al., 2010; Dall'Osto et al.,
83 2017; Kalkavouras et al., 2017), in urban areas intensive studies have started mainly in recent years
84 (Jeong et al., 2010; Minguillón et al., 2015; Peng et al., 2017; Németh et al., 2018). Early studies in
85 Birmingham, UK highlighted the connection of NPF events with solar radiation (Shi et al., 2001) and
86 a low condensation sink (Alam et al., 2003), a measure of pre-existing aerosol loading (Dal Maso et
87 al., 2002). The importance of a low condensation sink was further underlined by later studies, as being
88 one of the most influential variables in the occurrence of NPF in all types of environment (Wehner et
89 al., 2007; Park, Yum and Kim, 2015; Pikridas et al., 2015). An important contributor to many NPF
90 pathways is SO_2 (Woo et al., 2001; Berndt et al., 2006; Laaksonen et al., 2008), which in the presence
91 of solar radiation forms H_2SO_4 , often the main component of the initial clusters (Kuang et al., 2008;
92 Kulmala et al., 2013; Bianchi et al., 2016; Kirkby et al., 2016). Dall'Osto et al. (2013) pointed out
93 that the role of SO_2 is less significant in urban areas compared to rural and background areas. SO_2
94 concentration variability in urban areas was found to have a small impact on the frequency of NPF

95 events (Alam et al., 2003; Jeong et al., 2010), though it can have an effect on the number of particles
96 formed (Charron et al., 2007). Furthermore, Dall'Osto et al. (2018) in their research at 24 sites in
97 Europe, pointed out the different role SO₂ seems to play depending on its concentration, and that of
98 other species. Jayaratne et al. (2017) however found that in the heavily polluted environment of
99 Beijing, China, NPF events were more probable in sulphur rich conditions rather than sulphur poor.
100 Apart from its role in the initial formation of the clusters, H₂SO₄ seems to participate in the early
101 stages of growth of the newly formed clusters (Kulmala et al., 2005; Iida et al., 2008; Xiao et al.,
102 2015). In later stages of growth, low or extremely low volatility organic compounds (O'Dowd et al.,
103 2002; Laaksonen et al., 2008; Metzger et al., 2010; Kulmala et al., 2013; Tröstl et al., 2016; Dall'Osto
104 et al., 2018) appear to be more important, while the role of ammonium nitrate in particle growth is
105 also considered (Zhang et al., 2017). While in rural areas the organic compounds are mainly of
106 biogenic origin (Riccobono et al., 2014; Kirkby et al., 2016), in urban areas they mainly originate
107 from combustion processes (Robinson et al., 2007; Gentner et al., 2012). Many comparative studies
108 have reported higher growth rates in urban areas compared to background sites (Wehner et al., 2007;
109 Jeong et al., 2010; Salma, et al., 2016; Wang et al., 2017), as well as greater particle formation rates
110 (Salma, et al., 2016; Nieminen et al., 2018) and a higher frequency of NPF events (Peng et al., 2017),
111 which was attributed to the higher concentration of condensable species. Salma et al. (2014) however
112 reported fewer NPF events in the city centre of Budapest compared to the urban background, due to
113 the higher condensation sink. Due to the complexity of the conditions and mechanisms within an
114 urban area (Harrison, 2017), NPF events are harder to study and factors to be attributed. Increased

115 concentrations of particles in the size range 1.3 – 3 nm were measured at a kerbside site when
116 downwind from the road, following the trends in traffic-related nucleation mode particles, associating
117 them with traffic emissions and thus not resulting from homogeneous nucleation mechanisms
118 (Rönkkö et al., 2017; Hietikko et al., 2018), and studies in Barcelona, Spain (Dall'Osto et al., 2012;
119 Brines et al., 2014) and Leicester, U.K. (Hama et al., 2017), attributed a larger portion of nucleation
120 mode particles to vehicular emissions compared to photochemically induced nucleation. As the
121 condensation sink is higher within an urban environment, NPF events are less favoured. Their
122 occurrence is attributed to either ineffective scavenging or the higher growth rate of the newly formed
123 particles (Kulmala et al., 2017), when sufficient concentrations of precursors are present in the
124 atmosphere (Fiedler et al., 2005), as particle formation was found to take place on both event and
125 non-event days with variable intensity, though not always followed by survival or growth of the newly
126 formed particles, thus not qualifying as NPF events (Riipinen et al., 2007).

127

128 In this study, NPF events in three areas of different land use in the southern U.K. are analyzed. Studies
129 for NPF events have been conducted in the past for Harwell, Oxfordshire (Charron et al., 2007; 2008)
130 and the effect of NPF upon particle size distributions was also considered for N. Kensington, London
131 (Beddows et al., 2015). A combined study including all three sites has also been conducted, but in
132 the aspect of ultrafine particle variation (Von Bismarck-Osten et al., 2013). The present study is the
133 first to use a combined long term database for all three sites, focusing on the trends and conditions of
134 NPF events at these sites, as well as the first which identifies NPF events at the highly trafficked

135 Marylebone Road site, as up to this point ultrafine particles were attributed only to traffic (Charron
136 and Harrison, 2003; Dall'Osto et al., 2011). As in this study a rural and an urban background area are
137 studied alongside a kerbside site in the city of London in close proximity, the conditions and
138 development of NPF events in a mid-latitude European region are discussed in relation to the
139 influence of different local environments.

140

141 **2. DATA AND METHODS**

142 **2.1 Site Description and Data Availability**

143 This study analysed NPF events in three areas in the southern United Kingdom (Fig. 1). Harwell in
144 Oxfordshire, is located about 80 km west of the greater London area. The site is in the grounds of the
145 Harwell Science Centre in Oxfordshire ($51^{\circ} 34' 15''$ N, $1^{\circ} 19' 31''$ W) and is representative of a rural
146 background area; a detailed description of the site was given by Charron et al. (2013). North
147 Kensington is a suburban area in the western side of London, U.K, 4.5 km west of Marylebone Road.
148 The site is located in the grounds of Sion Manning School ($51^{\circ} 31' 15''$ N, $0^{\circ} 12' 48''$ W) and is
149 representative of the urban background of London. A detailed description of the site was given by
150 Bigi and Harrison (2010). Marylebone Road is located in the centre of London, U.K. The site is
151 located on the kerbside of Marylebone road ($51^{\circ} 31' 21''$ N; $0^{\circ} 9' 16''$ W), a very busy arterial route
152 within a street canyon. A more detailed description of the area can be found in Charron and Harrison
153 (2003).

154 At all three sites, seven years (2009 – 2015) of particle number size distributions in the range of 16.6
155 – 604 nm have been measured and recorded as 15-minute averages, using a Scanning Mobility
156 Particle Sizer (SMPS), comprised by an Electrostatic Classifier (EC, TSI model 3080) and a
157 condensation Particle Counter (CPC, TSI Model 3775), operated on behalf of the Department for
158 Environment, Food and Rural Affairs (DEFRA) in the U.K. At all sites the inlet air is dried, and
159 operation is in accord with the EUSAAR/ACTRIS protocol (Wiedensohler et al., 2012). These 15-
160 minute measurements were averaged to an hourly resolution. In Harwell there were 46930 hours of
161 available SMPS data (76.5% coverage), in N. Kensington 51059 (83.3% coverage) and at Marylebone
162 Road 45562 (74.3% coverage). Detailed data availability is found in Table S1. A free-standing CPC
163 (TSI model 3022A) also operated alongside for most of the years of the survey and was used to give
164 an estimate of particles in the 7-16.6 nm range by difference from the SMPS.

165

166 Additionally, air pollutants and other gas and particle chemical composition data (NO_x , SO_2 , SO_4^{2-} ,
167 Cl, Na, Mg, gaseous ammonia and VOCs) were extracted from the DEFRA website ([https://uk-
168 air.defra.gov.uk/](https://uk-air.defra.gov.uk/)); Daily measurements of particulate OC were also extracted from the DEFRA
169 website which are determined using the method described in the Annual report of the National
170 Physical Laboratory (Beccaceci et al., 2015). Meteorological data for Harwell and Heathrow airport
171 (used for N. Kensington and Marylebone road) were available from the Met Office, while solar
172 radiation data from Benson station (for Harwell) and Heathrow airport (for N. Kensington and
173 Marylebone Road), were extracted from the Centre for Environmental Data Analysis (CEDA) site

174 (<http://www.ceda.ac.uk>). Back trajectory data calculated using the HYSPLIT model (Draxler and
175 Hess, 1998), were extracted by the NOAA Air Resources Laboratory
176 (<https://ready.arl.noaa.gov/READYtransp.php>) and were processed using the Openair package for R
177 (Carslaw and Ropkins, 2012).

178

179 **2.2 Methods**

180 **2.2.1 NPF events selection**

181 The identification of the NPF event days was made by visual inspection of SMPS data, supplemented
182 with the use of CPC data to confirm the formation of a new mode of particles, using the criteria set
183 by Dal Maso et al. (2005). NPF events are considered when a distinctly new mode of particles which
184 appears in the size distribution at nucleation mode size, prevails for some hours and shows signs of
185 growth. Using these criteria, NPF events are classified into two classes, I and II depending on the
186 level of certainty. Class I events are further classified to Ia and Ib, with class Ia containing very clear
187 and strong particle formation events, while Ib contains less clear events. In this study the events of
188 class Ia only are considered as being the most suitable for analysing case studies of NPF events
189 (Figure S1). At this point it should be mentioned that due to the particle size range available, NPF
190 events in which new formed particles failed to grow beyond 16.6 nm (if any) could not be identified.
191 Bursts of new particles in the size range < 16.6 nm that were identified using the CPC data but did
192 not appear in the SMPS dataset were ignored as their development was unknown. This type of
193 development was rare and mainly found at the rural background site, occurring on a few days per

194 year mainly in summer. Its main feature was the short duration of the bursts compared to event days.
 195 In the urban sites, this type of development was almost non-existent. High time resolution data for
 196 gaseous pollutants and aerosol constituents was used to identify pollution events affecting particle
 197 concentrations and these were removed from the data analysis. This analysis took account of the fact
 198 that nanoparticle emissions from Heathrow Airport affect size distributions at London sites (Harrison
 199 et al., 2018), and such primary emission influences were not included as NPF events.

200

201 **2.2.2 Calculation of the condensation sink and growth rate**

202 For the calculation of the condensation sink the method proposed in Kulmala et al. (2001) was used
 203 in which the condensation sink is calculated as

204

$$205 \quad CS = 4\pi D \sum \beta_M r N \quad (1)$$

206

207 where r is the radius of the particles and N is the number concentration of the particles. D is the
 208 diffusion coefficient calculated (for $T = 293$ K and $P = 1013.25$ mbar) according to Polling et al.
 209 (2000):

210

$$211 \quad D_{vap} = 0.00143 \cdot T^{1.75} \frac{\sqrt{M_{air}^{-1} + M_{vap}^{-1}}}{P \left(D_{x,air}^{\frac{1}{3}} + D_{x,vap}^{\frac{1}{3}} \right)^2} \quad (2)$$

212

213 where P is air pressure, M is the molar mass and D_x is the diffusion volume for air and H_2SO_4 . β_M is
214 the Fuchs correction factor calculated as (Fuchs et al., 1971):

215

$$\beta_M = \frac{1 + K_n}{1 + \left(\frac{4}{3a} + 0.377\right)K_n + \frac{4}{3a}K_n^2} \quad (3)$$

217

218 where K_n is the relation of the particle diameter and the mean free path of the gas λ_m , called the
219 Knudsen number.

220

221 The growth rate of the particles on nucleation event days was also calculated as proposed by Kulmala
222 et al. 2012, using the formula

223

$$GR = \frac{D_{P_2} - D_{P_1}}{t_2 - t_1} \quad (4)$$

225

226 for the size range 16.6 – 50 nm. The number of points taken depended on the development of the
227 event and were considered from the start of the event until a) growth stopped, b) GMD reached 50
228 nm or c) the day ended (this cut-off was chosen as the development of an event in its later stages is
229 heavily biased by the local conditions, especially at the urban sites).

230

231 2.2.3 Calculation of the urban increment (U.I.)

232 The urban increment is defined as the ratio of the number concentration of particles below 20 nm for
233 event days to the average (for the period April – October, when the majority of the events take place)
234 for North Kensington to that at Harwell. This provides with a measure of the new particles formed in
235 each area in comparison to the average conditions, and is calculated by

$$236 \text{ U.I.} = \frac{NK_{\text{Nuc Max}} - NK_{\text{Bg}}}{HW_{\text{Nuc Max}} - HW_{\text{Bg}}} \quad (5)$$

237

238 where $NK_{\text{Nuc Max}}$ is the maximum concentration of particles below 20 nm found in the diurnal cycle
239 on event days (found at 13:00) and NK_{Bg} is the average mean concentration at the same time (same
240 for Harwell in the denominator).

241

242 2.2.4 Calculation of nucleation strength factor (NSF) and the P parameter

243 The Nucleation Strength Factor (NSF) was proposed by Salma et al. (2014) as a measure of the effect
244 nucleation events have in the composition of ultrafine particles in an area. Two factors were proposed.
245 First is the NSF_{NUC} . This is calculated as

246

$$247 \text{ NSF}_{\text{NUC}} = \frac{\left(\frac{N_{(\text{smallest size available}-100)}}{N_{(100-\text{largest size available})}} \right)_{\text{nucleation days}}}{\left(\frac{N_{(\text{smallest size available}-100)}}{N_{(100-\text{largest size available})}} \right)_{\text{non-nucleation days}}} \quad (6)$$

248

249 and provides of a measure of the concentration increment on nucleation days exclusively caused by
 250 new particle formation (NPF). The second factor is NSF_{GEN} calculated as

$$251 \quad NSF_{GEN} = \frac{\left(\frac{N_{\text{smallest size available}} - 100}{N_{100 - \text{largest size available}}} \right)_{\text{all days}}}{\left(\frac{N_{\text{smallest size available}} - 100}{N_{100 - \text{largest size available}}} \right)_{\text{non-nucleation days}}} \quad (7)$$

253 and gives a measure of the overall contribution of NPF on a longer span (Salma et al. 2017).
 254 The dimensionless survival parameter P, as proposed in Kulmala et al. (2017), was calculated as

$$255 \quad P = \frac{CS'}{GR'}$$

257 where CS' = CS/(10⁻⁴ s⁻¹) and GR' = GR/(1 nm hour⁻¹). CS and GR values used were calculated with
 258 the methods mentioned at 2.2.2. An increased P parameter is an indication that a smaller percentage
 259 of newly formed particles will survive to greater sizes. Hence this is the inverse of particle
 260 survivability, and values of P<50 are typically required for NPF in clean or moderately polluted
 261 environments, although higher values of P are observed in highly polluted atmospheres (Kulmala et
 262 al, 2017).

RESULTS AND DISCUSSION

3.1 NPF Events in the Background Areas

3.1.1 Conditions and trends of NPF events

The number of NPF event days for each site per year, those that took place simultaneously at both urban and rural background sites, as well as those events that took place at all three sites simultaneously appear in Table 1. Given that overall data recovery was in the range of 74-83%, results from individual years are unreliable, but the seven-year runs should average out most of the effects of incomplete data recovery. The number of events is similar for Harwell and N. Kensington, with a frequency of about 7% of all days with data. There is a clear seasonal variation favouring summer and spring (Figure 2) for both areas of the study. A similar pattern of variation was found for N. Kensington by Beddows et al. (2015). In general, higher solar radiation, lower relative humidity, low cloud cover and higher pressure conditions, lower concentrations of pollutants as well as lower condensation sink are found when NPF events took place in all areas (Figure S2), as was also reported by Charron et al. (2007) for Harwell. While SO₂ is one of the main factors for NPF events to occur, concentrations are lower when events take place. This is indicative that SO₂ concentrations in these areas are sufficient for events to take place, and higher concentrations are likely to be associated with higher pollution and a higher condensation sink. The proxy for [H₂SO₄] was calculated for the background sites using the method outlined in Petäjä et al., (2009) and was found to be higher on event days for both background sites (results not included). This indicates the possible positive effect of increased concentrations of H₂SO₄ in the occurrence of NPF events as well as, since SO₂

287 concentrations were found lower, the increased role of either the solar radiation (via the formation of
288 OH radical) or the reduced condensation sink to its formation. For the case of gaseous ammonia
289 (results not included) for Harwell where data was available, as there was no distinct variation found
290 between event and non-event days, but as the concentration of ammonia in the U.K. is in the range of
291 few ppb (Sutton et al., 1995), it is sufficient according to ternary nucleation theory (Korhonen et al.,
292 1999) for NPF events not to be limited by ammonia. The average growth rate for Harwell was found
293 to be 3.4 nm h^{-1} , within the range given by Charron et al. (2007) and higher at N. Kensington at 4.2
294 nm h^{-1} , a trend found for all seasons (Figure 3). The increased growth rate in the urban area can be
295 related to the greater presence of organic matter and other condensable species. In both areas NPF
296 events had higher growth rates in summer than in spring, as was also found in previous studies
297 (Kulmala et al., 2004; Nieminen et al., 2018). This may be associated with the higher concentration
298 of organic compounds emitted by trees during summer (Riipinen et al., 2007), or faster oxidation
299 rates due to higher concentrations of hydroxyl radical and ozone (Harrison et al., 2006).

300

301 About 45% of the events took place simultaneously in both background areas. These events are
302 characterized as regional, as NPF took place on a larger scale, regardless of the local conditions of
303 the given area. In this case, meteorological conditions were even clearer, indicative of the greater
304 dependence of regional events on synoptic conditions rather than local. While most chemical
305 constituents were also lower in concentration during regional events, different patterns were found
306 for organic compounds and sulphate for each background area. In Harwell sulphate was higher during

307 regional events, while in N. Kensington organic compounds were higher during regional events. This
308 may be indicative of the variable role that specific chemical species have in condensational
309 nanoparticle growth (Yue et al., 2010). In all cases though, the concentrations of these species were
310 lower compared to the average conditions. Despite these differences, the growth rate of particles was
311 found to be higher for local events in N. Kensington (4.4 nm h^{-1}) compared to regional events (3.9
312 nm h^{-1}), though within the margin of uncertainty. In Harwell, no difference was found in the growth
313 rate between regional and local events.

314

315 **3.1.2 Urban increment and particle development**

316 The urban environment, depending on the conditions, may have a positive or negative effect in the
317 number of the particles formed and their consequent survival and growth. Both Harwell and N.
318 Kensington are in background areas, rural and urban respectively. As a result, while the
319 concentrations of pollutants are higher in N. Kensington than Harwell, their effect is smaller
320 compared to that of Marylebone Road. A comparison of the particles smaller than 20 nm, gives insight
321 into the formation and survival of the newly formed particles in the early stages. Calculating the urban
322 increment (equation 5) using the two background sites showed around 20% more particles of size 16
323 - 20 nm in N. Kensington than Harwell for event days, an increment that is even stronger when solely
324 local events are considered (Figure 4). As the sizes of the particles in the calculation are relatively
325 large and due to the higher condensation sink found in N. Kensington, this increment is expected to
326 be larger for smaller size particles. A possible explanation for this result may be the greater

327 concentration of organic compounds which is observed in N. Kensington, as discussed earlier, which
328 leads to more rapid formation of secondary condensable species that enhances the nucleation process
329 in the more polluted area.

330

331 Considering the local events, most of the pollutant concentration data available appear to be higher
332 which is reflected in the condensation sink as well. The role of the polluted background appears to be
333 decisive in the further growth of the newly formed particles, especially for Harwell. This, at both sites
334 causes the number of particles of greater size to be smaller for the later hours in the days of local
335 events (Figure S3). Another possible reason for this difference in the larger size ranges can be the
336 higher concentration of organic content on the days of regional events at N. Kensington (as discussed
337 earlier). On the other hand, for Harwell all hydrocarbons with available data are lower throughout the
338 day (apart from ethane) during regional events. Unlike N. Kensington, at Harwell particles smaller
339 than 20 nm as well as the growth rate of the newly formed particles are almost the same for regional
340 and local events.

341

342 The calculation of the increment in Marylebone Road provided negative results; particles smaller than
343 20 nm were less abundant on event days compared to the average, throughout the day. This is due to
344 the fact that Marylebone road is heavily affected by traffic pollution and on average, conditions do
345 not promote NPF events due to the high condensation sink, unless clear conditions prevail, which are
346 also associated with a low particle load.

347 **3.2 NPF Events at Marylebone Road**

348 For many years, NPF events were thought not to take place in heavily polluted urban areas, as the
349 effect of the increased condensation sink was considered crucial in suppressing the formation and
350 growth of new particles. Recent long term analyses have shown this is not the case and nowadays an
351 increasing number of studies confirm the occurrence of NPF events in urban areas. In this study, for
352 the same period of seven years as for the two background areas, NPF events were found to occur for
353 6.1% of days at Marylebone Road, lower than in the background areas. Though, due to the particle
354 size range available there cannot be a definitive answer to whether the formation of the particles takes
355 place in the specific locality of the sampling site, due to the observed increase in particle
356 concentrations in the range 7 – 16 nm (provided by the CPC data) and the increased growth rates
357 found in urban areas in general, it can be assumed that the formation takes place either in the area of
358 the measuring site or in its close vicinity, while the growth of the particles persists in the area for
359 several hours, despite the high condensation sink. Seasonal variation is similar to that at the
360 background sites, but day of the week variation is stronger at Marylebone Road further favouring
361 weekends (Figure S4), as on these days traffic intensity is lower.

362

363 In general, similar conditions found to affect NPF events at the background sites are also found at
364 Marylebone Road, despite a much larger condensation sink. (Figure S2). As a result, less particles of
365 size smaller than 20 nm were found on NPF event days than the average for the site, as the sum of
366 background particles plus those formed on these days were less than that on an average day. The

367 growth rate of the newly formed particles (5.5 nm h^{-1}), is higher than that of the background sites
368 which is in agreement with the findings in the study of the background areas on the possible role of
369 the condensable species, the concentrations of which are even greater at the urban kerbside. About
370 15% of NPF event days at Marylebone Road presented particle shrinkage after the initial growth; the
371 study of these cases though is outside of the context of the present work. At Marylebone Road, the
372 number of NPF days which were common with the background sites was fewer, as local conditions
373 (high condensation sink) are detrimental to the occurrence of NPF events and thus the days of regional
374 events including Marylebone Road were separately studied for this site. The regional event days that
375 were common for all three sites were 37 (31% of events at Marylebone Road) (Table 1). As with the
376 other two areas, the growth rate is higher during local events, but the conditions are mixed, with lower
377 concentrations of sulphate and organic compounds but higher SO_2 , NO_x and elemental carbon. The
378 relationship with higher wind speed (mainly western) (Figure S6), solar radiation (which results in
379 greater H_2SO_4 formation) and lower relative humidity, indicate the stronger relation of the regional
380 events with synoptic conditions than the local events in the heavily polluted environment of
381 Marylebone Road.

382

383 **3.3 Connection of NPF Events with Incoming Air Masses**

384 **3.3.1 Air mass back trajectory clustering and connection with NPF events**

385 The origin of the air masses plays a very important role in the occurrence of NPF events. Air masses
386 of different origins have different characteristics. Back trajectories provide excellent insight into the

387 source of the air masses. Air mass back trajectories were calculated both for all days and for NPF
388 event days for each site separately. This analysis gives a view of the frequency of NPF events within
389 different air mass types. The initial air mass back trajectory clustering ended up with an optimal
390 solution of 9 clusters of different air masses. As many of these clusters had similar characteristics and
391 origin, solutions with fewer clusters were attempted. As the number of clusters was decreasing
392 clusters became a mixture of different origins, thus making the distinction of different sources harder.
393 As a result, the method chosen was to merge clusters of similar origin and characteristics, which kept
394 the detail of the large number of clusters and made the separation of the different origins more distinct.
395

396 The resulting four merged clusters (Figure 5), using the characterisation proposed by McIntosh et al.
397 (1969) are:

- 398 • An **Arctic** cluster, which originates mainly from the northerly sector. It occurs about 10% of the
399 time and consists of cold air masses, which either passed over northern parts of the U.K. or
400 through the Irish Sea.
- 401 • A **Tropical** cluster, which originates from the central Atlantic. It occurs 25% of the time and
402 contains warmer air masses. A small percentage of this cluster contains masses that have passed
403 over countries south of the U.K. Even though these days were more polluted, the clustering
404 method was unable to clearly distinguish these days as it does not take into account particle
405 numbers or composition, even when the 9-cluster solution was applied.

- 406 • A **Polar** cluster, which originates from the north Atlantic. It is the most common type of air mass
407 arriving in the areas of study and occurs about 40% of the time bringing fast moving, “clean” air
408 masses with increased marine components (Cl, Na, Mg) from the west. This cluster also contains
409 airmasses that have passed through Ireland, though an effect on particle size and chemical
410 composition is not distinct.
- 411 • A **Continental** cluster, which originates from the east. It occurs about 25% of the time and
412 consists mainly of slow moving air masses, originating from the London area (for the background
413 areas) and/or continental Europe. It has higher concentrations of most pollutants as well as the
414 highest condensation sink.

415

416 The occurrence of each air mass class for average and event days for Harwell and London (both sites)
417 can also be found in Figure 5, while their main characteristics for each site can be found in Table S2.
418 Though in this case the air mass grouping for each site was done in a different analysis, the resulting
419 groups are almost identical in their characteristics and frequency, as the sites are close to each other.
420 The Polar cluster is the one prevailing on both average and event days. This consists of clean fast-
421 moving air masses originating mainly from mid and high latitudes of the Atlantic, and this cluster
422 presents favourable conditions for NPF events. The association of NPF events with air masses from
423 the mid-Atlantic at N. Kensington was also found by Beddows et al. (2015). Cool Arctic air masses
424 on average are not clean as they may have passed over the northern U.K. The event days associated
425 with this air mass type have the lowest concentrations of the pollutants within available data for all

426 areas. The increased percentage of events with this air mass at all sites indicates that lower
427 temperatures, in a clear atmosphere with sufficient solar radiation are favourable for NPF events as
428 found in previous studies (Napari et al., 2002; Jeong et al., 2010; Kirkby et al., 2011). A similar trend
429 of increased probability with polar and arctic maritime air masses was also found for Hyytiälä,
430 Finland by Nilsson et al. (2001). Tropical air masses have a lower probability for NPF events, which
431 is associated with the fact that a number of these days are associated with air masses which have
432 passed from continental areas south of the U.K. (France, Spain etc.). Specifically for Marylebone
433 Road the NPF probability is a lot lower (11% versus 17% for N. Kensington and 20% for Harwell).
434 This is due to the fact that these air masses are more related to southerly winds which, in Marylebone
435 Road are associated with a street canyon vortex which causes higher pollutant concentrations at this
436 site. Finally, the Continental cluster presents the lowest probability for NPF events. The air masses
437 in this group originate from continental Europe and for the background areas in most cases have
438 passed over the London region as well. This results in both a higher condensation sink and
439 concentration of pollutants, which limits the number of days with favourable conditions for NPF
440 events. Growth rate for all sites though appears to be higher for air masses originating from more
441 polluted areas (Figure 6), which appear to enhance the growth process due to containing a higher
442 concentration of condensable species (after oxidation).

443

444

445

446 3.3.2 Variability of the origin of the air masses on NPF events

447 As both background sites are relatively close to each other (about 80 km) and had similar number of
448 event days, a combined clustering of back trajectories for the event days (only) in these two areas was
449 attempted. This would provide an insight into the origin of air masses for local and regional events,
450 as well as the conditions for these air masses. The data for local N. Kensington events and both local
451 and regional events in Harwell were clustered together and the results along with the characteristics
452 of the air mass clusters are found in Figure S5.

453

454 Cluster C3, which is placed between C2 and C4 among those originating from the Atlantic Ocean,
455 has the highest percentage for both area specific and regional events. Specifically, for regional events
456 the percentage is over 35%, much higher compared to all other, showing a clear “preference” of
457 regional events for cleaner and faster moving air masses from mid-latitudes of the Atlantic Ocean.
458 This “preference” explains the lower production and growth rate of the new particles found for
459 regional events, compared to local ones, as for air masses from this area lower organic carbon and
460 SO₂ concentrations were found at both sites in this study. Cluster C5, originating straight from the
461 north but representing air masses that have crossed the Irish Sea and have not extensively gone over
462 land presents a similar case. These cold and clean air masses are associated with a low growth rate
463 and consequently low survivability of the newly formed particles. Local events for both sites apart
464 from those in Cluster C3 are highly associated with Clusters C1 and C2. C1, which contains slow and
465 polluted air masses, presents the highest growth rate and as a result high particle survivability, as

466 given by the P parameter (see later). On the other hand, C2 which consists of warm and moist air
467 masses from lower latitudes is the least common for regional events and presents high growth rate
468 and survival probability of the particles. Apart from the weak relation found with particulate organic
469 carbon concentrations and growth rate (Figure S5), there appears to be an inverse relation between
470 the temperature and survivability of the particles. Warmer air masses seem to be related to higher
471 particle survival probability, which may be attributable to greater growth rates as temperature
472 increases (Yli-Juuti et al., 2011).

473

474 **3.4 Nucleation Strength Factor (NSF)**

475 The NSF (equations 6 and 7) is used to describe the effect nucleation events have on the number of
476 particles at a site. The values of NSF for each site and for seasons spring and summer are shown in
477 Table 2. The decrease of the contribution of NPF events to particle number, moving from the rural
478 area to the kerbside was also found in previous studies (Salma et al., 2014; 2017). This is explained
479 by the increased contribution to the particle number concentrations of other sources, mainly
480 combustion in the urban environment, compared to rural areas. Apart from this trend, in the
481 background areas the increase of N_{16-100} was greater in spring than summer. This effect seems stronger
482 in the urban background area compared to the rural, as in that area the variability of N_{16-100} is greater
483 for event days compared to that of the rural area. On the other hand, the contribution of NPF events
484 in the longer span, as is illustrated by the NSF_{GEN} appears to favour summer for all areas, showing
485 the increased formation and survivability of particles in this season.

486 For Marylebone Road the result for the increase of the N_{16-100} is greater in summer than in spring, in
487 contrast to what was found for the background sites. This is due to the fact that in summer the traffic
488 intensity is decreased, giving the contribution from NPF events a stronger effect compared to the
489 other sources. The very small increase found on NPF events in Marylebone Road, with a factor of
490 just 1.26, a lot lower than that found in the urban area of Seoul, South Korea (Park et al., 2015), is
491 indicative of the reduced effect of NPF events in an area which is heavily affected by traffic, as also
492 pointed out by Von Bismarck-Osten et al. (2013) in their study on particle composition in Marylebone
493 Road.

494

495 **3.5 The Survival Parameter P**

496 The average values of the P parameter for each of the areas of this study are 10.5 for Harwell, 15.8
497 for N. Kensington and 28.9 for Marylebone Road. The values found put Marylebone Road to the
498 upper end of heavily polluted areas in Europe, North Kensington to the same level as many other
499 urban areas in Europe, while Harwell had somehow higher values compared to other rural background
500 areas in Europe, as calculated by Kulmala et al. (2017). The seasonal, air mass origin and local versus
501 regional variations can be found in Figure 7 (winter is excluded due to very low number of events).
502 While the increasing trend of the P parameter as we move from rural background to kerbside was
503 expected, it can be seen that there is a clear seasonal pattern in all three areas, with summer having
504 the lowest P parameter (greatest survivability) compared to the other two seasons. This is associated
505 with the higher growth rate found in summer for all areas of this study, as the differences in the

condensation sink on event days are negligible between seasons. The case is similar for regional and local events. The result per air mass origin is related to the different conditions and parameters of each incoming air mass in each area. For example, the higher P parameter for Tropical air masses at Marylebone Road, is associated with the higher condensation sink found for this kind of air masses, due to the street canyon effect which is specific for Marylebone Road for southerly wind directions with which these air masses are mainly related, while the higher values for the rather clean Arctic air masses for the other two areas are associated with the lower growth rates found for this kind of air mass in these areas. The more polluted Continental air masses seem to have a different effect for rural and urban areas. Their higher condensation sinks and concentrations of pollutants have a negative effect on P-values for the rural site and a positive effect at the urban sites. The exact opposite is found for the cleaner air masses of the Polar cluster, which appear to result in reduced P-values of the newly formed particles at the urban sites. This is related to the lower condensation sink associated with this air mass type.

519

520 **4. CONCLUSIONS**

Seven years of particle size distributions in the range 16.6 – 604 nm and other meteorological and chemical composition data from three distinct areas (regional background, urban background, kerbside) in the southern U.K. were analysed and the conditions associated with NPF events were studied. NPF events were found to occur on about 7% of days at background sites and less at the kerbside site. The conditions on event days for all three areas were similar, with clear atmospheric

526 conditions and a lower condensation sink. While the condensation sink appears to be the most
527 important factor limiting NPF events at the kerbside site, SO₂ was found to have smaller
528 concentrations on event days for all areas, which indicates that either on average it is in sufficient
529 concentrations for NPF events to occur, or that other variables that participate in the production
530 mechanism of H₂SO₄ are more important. The growth rate of the newly formed particles increases
531 from the rural site to the kerbside and is greater in summer compared to other seasons for all three
532 sites. Almost half of the NPF events at the rural and urban background sites were found to happen
533 simultaneously. In these cases, the atmospheric conditions were cleaner, which resulted in slower
534 growth rates. While most of the chemical species available were at lower concentrations in regional
535 events, a difference in the behaviour with respect to sulphate and organic compounds was found
536 between the two background site types.

537

538 The prevailing origin of air masses in the southern U.K. is from mid and high latitudes of the Atlantic
539 Ocean. These fast-moving air masses present an increased probability for NPF to occur. The case is
540 similar for the cooler and cleaner arctic air masses, while air masses from the tropics and continental
541 Europe, having greater pollutant content, have decreased NPF probability, but a higher growth rate
542 of particles when NPF events occurred. Regional events appear to be more associated with cleaner
543 air masses, presenting a smaller growth rate and condensation sink compared to local events. The
544 difference in growth rate is probably related to the greater content of condensable species; a positive
545 relation of particle survival probability with temperature was also found.

546 Comparing the background areas in this study, particles of 16-20 nm were found to be about 20%
547 greater in concentration (above long-term average) on NPF event days at the urban background site
548 compared with the rural site. This is associated with a higher abundance of condensable species in
549 the urban environment, which enhances the nucleation and growth process. This effect though is
550 limited as particle size increases and NPF events have a greater effect on the overall $N_{<100\text{ nm}}$ in the
551 rural areas, compared to urban, as calculated by the NSF. The effect becomes even smaller at the
552 kerbside as the number of background particles emitted by traffic is a lot greater.

553

554 The occurrence of NPF events at the highly polluted Marylebone Road site is at first sight surprising
555 given the elevated condensation sink. This must be counteracted by an abundance of condensable
556 material, which is surprising given the generally modest rate of atmospheric oxidation processes in
557 comparison to residence times in a street canyon (Harrison, 2017). However, Giorio et al. (2015),
558 using Aerosol Time-of-Flight Mass Spectrometry, reported rapid chemical processes within the
559 Marylebone Road street canyon leading to production of secondary particulate matter from road
560 traffic emissions. They postulated that this resulted from very local gas to particle conversion from
561 vehicle-emitted pollutants. Condensation of such reaction products upon pre-existing particles could
562 explain the enhanced particle growth rates observed at Marylebone Road (Figure 3).

563

564 Finally, particle survival probability was found to decrease moving from rural to urban areas. While
565 formation and initial growth of new particles is increased in urban areas, their survivability reduces

566 as their size increases. The probability of particles to survive to greater sizes was found to be increased
567 in summer for all areas, which is also explained by the higher growth rate. The probability is also
568 different depending upon the origin of the air masses and is related to conditions specific for each
569 area.

570

571 In the present work, the effects of atmospheric conditions upon the NPF process are studied. NPF is
572 a complex process, highly affected by meteorological conditions (local and synoptic), the chemical
573 composition as well as the pre-existing conditions in an area. For this reason, the study of NPF events
574 in one area cannot provide safe assumptions for other areas, as the mixture of conditions found in
575 different places is unique and alters the occurrence and development of NPF events. Thus, more
576 studies on the conditions and the trends in NPF events should be conducted to better understand the
577 effect of the numerous variables that affect those processes.

578

579 **DATA AVAILABILITY**

580 Data supporting this publication are openly available from the UBIRA eData repository at
581 <https://doi.org/10.25500/edata.bham.00000307>.

582

583

584

585

586 **AUTHOR CONTRIBUTIONS**

587 This study was conceived by MD and RMH who also contributed to the final manuscript. The data
588 analysis was carried out by DB with guidance from DCSB, and DB also prepared the first draft of
589 the manuscript. FDP provided advice on the analysis.

590

591 **COMPETING INTERESTS**

592 The authors have no conflict of interests.

593

594 **ACKNOWLEDGEMENT**

595 The authors acknowledge financial support (to DCSB) from the National Environment Research
596 Council's funding of the National Centre for Atmospheric Science (NCAS) (Grant Number
597 R8/H12/83/011).

598

599 REFERENCES

- 600 Alam, A., Shi, J. P. and Harrison, R. M.: Observations of new particle formation in urban air, *Journal*
601 *of Geophysical Research: Atmospheres*, 108, 4093–4107, doi:10.1029/2001JD001417, 2003.
- 602
- 603 Atkinson, R. W., Fuller, G. W., Anderson, H. R., Harrison, R. M. and Armstrong, B.: Urban ambient
604 particle metrics and health: A time-series analysis, *Epidemiology*, 21, 501–511, 2010.
- 605
- 606 Beccaceci, S., McGhee, E., Robins, C., Butterfield, D., Tompkins, J., Quincey, P., Brown, R., Green,
607 D., Tremper, A., Priestman, M., Font Font, A.: Airborne particulate concentrations and numbers in
608 the United Kingdom (phase 3); Annual report 2015, available at [http://uk-](http://uk-air.defra.gov.uk/library/reports?section_id=13)
609 [air.defra.gov.uk/library/reports?section_id=13](http://uk-air.defra.gov.uk/library/reports?section_id=13)
- 610
- 611 Beddows, D. C. S., Harrison, R. M., Green, D. C., and Fuller, G. W.: Receptor modelling of both
612 particle composition and size distribution from a background site in London, UK, *Atmos. Chem.*
613 *Phys.*, 15, 10107-10125, 2015.
- 614
- 615 Berndt, T., Böge, O., and Stratmann, F.: Formation of atmospheric H₂SO₄H₂O particles in the
616 absence of organics: A laboratory study, *Geophys. Res. Lett.*, 33, 2–6, 2006.
- 617
- 618 Bianchi, F., Trostl, J., Junninen, H., Frege, C., Henne, S., Hoyle, C. R., Molteni, U., Herrmann, E.,
619 Adamov, A., Bukowiecki, N., Chen, X., Duplissy, J., Gysel, M., Hutterli, M., Kangasluoma, J.,
620 Kontkanen, J., Kurten, A., Manninen, H. E., Munch, S., Perakyla, O., Petaja, T., Rondo, L.,
621 Williamson, C., Weingartner, E., Curtius, J., Worsnop, D. R., Kulmala, M., Dommen, J., and
622 Baltensperger, U.: New particle formation in the free troposphere: A question of chemistry and
623 timing, *Science*, 352, 1109–1112, 2016.
- 624
- 625 Bigi, A. and Harrison, R. M.: Analysis of the air pollution climate at a central urban background site,
626 *Atmos. Environ.*, 44, 2004–2012, 2010.
- 627
- 628 Brines, M., Dall'Osto, M., Beddows, D. C. S., Harrison, R. M., and Querol, X.: Simplifying aerosol
629 size distributions modes simultaneously detected at four monitoring sites during SAPUSS, *Atmos.*
630 *Chem. Phys.*, 14, 2973–2986, 2014.
- 631
- 632 Carslaw, D. C. and Ropkins, K.: openair — An R package for air quality data analysis, *Environ.*
633 *Modell. Softw.*, 27–28, 52–61, 2012.
- 634
- 635 Charron, A., Birmili, W., and Harrison, R. M.: Factors influencing new particle formation at the rural
636 site, Harwell, United Kingdom, *J. Geophys. Res., Atmospheres*, 112,
637 doi:10.1029/2007JD0084252007.

638 Charron, A., Birmili, W., and Harrison, R. M.: Fingerprinting particle origins according to their size
639 distribution at a UK rural site, *J. Geophys. Res., Atmospheres*, 113, D07202,
640 doi:10.1029/2007JD008562, 2008.

641

642 Charron, A., Degrendele, C., Laongsri, B., and Harrison, R. M.: Receptor modelling of secondary
643 and carbonaceous particulate matter at a southern UK site, *Atmos. Chem. Phys.*, 13, 1879–1894,
644 2013.

645

646 Charron, A. and Harrison, R. M.: Primary particle formation from vehicle emissions during exhaust
647 dilution in the roadside atmosphere, *Atmos. Environ.*, 37, 4109–4119, 2003.

648

649 Dal Maso, M., Kulmala, M., Lehtinen, K. E. J., Mäkelä, J. M., Aalto, P., and O’Dowd, C. D.:
650 Condensation and coagulation sinks and formation of nucleation mode particles in coastal and boreal
651 forest boundary layers, *J. Geophys. Res., Atmospheres*, 107, doi: 10.1029/2001JD001053, 2002.

652

653 Dal Maso, M., Kulmala, M., Riipinen, I., Wagner, R., Hussein, T., Aalto, P. P., and Lehtinen, K. E.
654 J.: Formation and growth of fresh atmospheric aerosols: Eight years of aerosol size distribution data
655 from SMEAR II, Hyytiälä, Finland, *Boreal Environ. Res.*, 10, 323–336, 2005.

656

657 Dall’Osto, M., Beddows, D. C. S., Asmi, A., Poulain, L., Hao, L., Freney, E., Allan, J. D.,
658 Canagaratna, M., Crippa, M., Bianchi, F., de Leeuw, G., Eriksson, A., Swietlicki, E., Hansson, H. C.,
659 Henzing, J. S., Granier, C., Zemannova, K., Laj, P., Onasch, T., Prevot, A., Putaud, J. P., Sellegri, K.,
660 Vidal, M., Virtanen, A., Simo, R., Worsnop, D., O’Dowd, C., Kulmala, M., and Harrison, R. M.:
661 Novel insights on new particle formation derived from a pan-european observing system, *Sci. Rep.*,
662 8, 1482, 2018.

663

664 Dall’Osto, M., Beddows, D. C. S., Pey, J., Rodriguez, S., Alastuey, A., M. Harrison, R., and Querol,
665 X.: Urban aerosol size distributions over the Mediterranean city of Barcelona, NE Spain, *Atmos.*
666 *Chem. Phys.*, 12, 10693–10707, 2012.

667

668 Dall’Osto, M., Querol, X., Alastuey, A., O’Dowd, C., Harrison, R. M., Wenger, J., and Gómez-
669 Moreno, F. J.: On the spatial distribution and evolution of ultrafine particles in Barcelona, *Atmos.*
670 *Chem. Phys.*, 13, 741–759, 2013.

671

672 Dall’Osto, M., Thorpe, A., Beddows, D. C. S., Harrison, R. M., Barlow, J. F., Dunbar, T., Williams,
673 P. I., and Coe, H.: Remarkable dynamics of nanoparticles in the urban atmosphere, *Atmos. Chem.*
674 *Phys.*, 11, 6623–6637, 2011.

675

676 Dall’Osto, M., Beddows, D. C. S., Tunved, P., Krejci, R., Ström, J., Hansson, H. C., Yoon, Y. J.,
677 Park, K. T., Becagli, S., Udisti, R., Onasch, T., Ódowd, C. D., Simó, R., and Harrison, R. M.: Arctic

678 sea ice melt leads to atmospheric new particle formation, *Sci.Rep.*, 7, 0–10, 2017.
679
680
681 Dameto de España, C., Wonaschütz, A., Steiner, G., Rosati, B., Demattio, A., Schuh, H. and
682 Hitzenberger, R.: Long-term quantitative field study of New Particle Formation (NPF) events as a
683 source of Cloud Condensation Nuclei (CCN) in the urban background of Vienna, *Atmos. Environ.*,
684 164, 289–298, 2017.
685
686 Davidson, C. I., Phalen, R. F., and Solomon, P. A.: Airborne particulate matter and human health: A
687 review, *Aerosol Sci, Technol.*, 39, 737–749, 2005.
688
689 Draxler, R. R., and Hess, G. D.: An Overview of the HYSPLIT_4 Modelling System for Trajectories,
690 Dispersion, and Deposition, *Australian Meteorolog. Mag.*, 47, 295–308, 1998.
691
692 Ehn, M., Vuollekoski, H., Petäjä, T., Kerminen, V.-M., Vana, M., Aalto, P., de Leeuw, G., Ceburnis,
693 D., Dupuy, R., O’Dowd, C. D., and Kulmala, M.: Growth rates during coastal and marine new particle
694 formation in western Ireland, *J. Geophys. Res.*, 115, D18218,
695 <http://dx.doi.org/10.1029/2010JD014292>, 2010.
696
697 Fiedler, V., Dal Maso, M., Boy, M., Aufmhoff, H., Hoffmann, J., Schuck, T., Birmili, W., Arnold,
698 F., and Kulmala, M.: The contribution of sulphuric acid to atmospheric particle formation and growth:
699 a comparison between boundary layers in Northern and Central Europe, *Atmos. Chem. Phys. Discuss.*
700 5, 573–605, 2005.
701
702 Fuchs, N. A. and Sutugin, A. G.: Highly Dispersed Aerosols, *Foreign Sci. and Technol. Center*, 1–
703 86, 1971.
704
705 Gentner, D. R., Isaacman, G., Worton, D. R., Chan, A. W. H., Dallmann, T. R., Davis, L., Liu, S.,
706 Day, D. A., Russell, L. M., Wilson, K. R., Weber, R., Guha, A., Harley, R. A., and Goldstein, A. H.:
707 Elucidating secondary organic aerosol from diesel and gasoline vehicles through detailed
708 characterization of organic carbon emissions, *Proc. Natl. Acad. Sci.*, 109, 18318–18323, 2012.
709
710 Hama, S. M. L., Cordell, R. L., Kos, G. P. A., Weijers, E. P., and Monks, P. S.: Sub-micron particle
711 number size distribution characteristics at two urban locations in Leicester, *Atmos. Res.*, 194, 1–16,
712 2017.
713
714 Harrison, R. M., Beddows, D. C. S., Alam, M. S., Singh, A., Brean, J., and R. Xu: Interpretation of
715 Particle number size distributions measured across an urban area during the FASTER campaign, in
716 preparation, 2018.
717

718 Harrison, R. M.: Urban atmospheric chemistry: a very special case for study, *npj Climate and Atmos.*
719 *Sci.*, 1, 5, 2017.

720

721 Harrison, R. M., Shi, J. P., Xi, S., Khan, A., Mark, D., Kinnersley, R., and Yin, J.: Measurement of
722 number, mass and size distribution of particles in the atmosphere, *Philos. Trans. A. Math. Phys. Eng.*
723 *Sci.*, 358, 2567–2580, 2000.

724

725 Harrison, R. M. and Yin, J.: Particulate matter in the atmosphere: Which particle properties are
726 important for its effects on health?, *Sci. Tot. Environ.*, 249, 85–101, 2000.

727

728 Harrison, R.M., Yin, J., Tilling, R.M., Cai, X., Seakins, P.W., Hopkins, J.R., Lansley, D.L.,
729 Lewis, A.C., Hunter, M.C., Heard, D.E., Carpenter, L.J., Creasey, D.C., Lee, J.D., Pilling, M.J.,
730 Carslaw, N., Emmerson, K.M., Redington, A., Derwent, R.G., Ryall, D., Mills G., and Penkett, S.A.,
731 Measurement and Modelling of Air Pollution and Atmospheric Chemistry in the UK West
732 Midlands Conurbation: Overview of the PUMA Consortium Project, *Sci. Tot. Environ.*, 360, 5-25
733 2006.

734

735 Hietikko, R., Kuuluvainen, H., Harrison, R. M., Portin, H., Timonen, H., Niemi, J. V., Ronkko, T.:
736 Diurnal variation of nanocluster aerosol concentrations and emission factors in a street canyon,
737 *Atmos. Environ.*, 189, 98-106, 2018.

738

739 Iida, K., Stolzenburg, M. R., McMurry, P. H., and Smith, J. N.: Estimating nanoparticle growth rates
740 from size-dependent charged fractions: Analysis of new particle formation events in Mexico City, *J.*
741 *Geophys. Res. Atmospheres*, 113, D05207, doi:10.1029/2007JD009260, 2008.

742

743 Jayaratne, R., Pushpawela, B., He, C., Li, H., Gao, J., Chai, F., and Morawska, L.: Observations of
744 particles at their formation sizes in Beijing, China, *Atmos. Chem. Phys.*, 17, 8825–8835, 2017.

745

746 Jeong, C.-H., Evans, G. J., McGuire, M. L., Chang, R. Y.-W., Abbatt, J. P. D., Zeromskiene, K.,
747 Mozurkewich, M., Li, S.-M., and Leitch, W. R.: Particle formation and growth at five rural and
748 urban sites, *Atmos. Chem. Phys.*, 10, 7979–7995, 2010.

749

750 Kalkavouras, P., Bossioli, E., Bezantakos, S., Bougiatioti, A., Kalivitis, N., Stavroulas, I.,
751 Kouvarakis, G., Protonotariou, A. P., Dandou, A., Biskos, G., Mihalopoulos, N., Nenes, A., and
752 Tombrou, M.: New particle formation in the southern Aegean Sea during the Etesians: Importance
753 for CCN production and cloud droplet number, *Atmos. Chem. Phys.*, 17, 175–192, 2017.

754

755 Kecorius, S., Kivekäs, N., Kristensson, A., Tuch, T., Covert, D. S., Birmili, W., Lihavainen, H.,
756 Hyvärinen, A. P., Martinsson, J., Sporre, M. K., Swietlicki, E., Wiedensohler, A., and Ulevicius, V.:
757 Significant increase of aerosol number concentrations in air masses crossing a densely trafficked sea

758 area, *Oceanologia*, 58, 1–12, 2016.

759

760 Kelly, F. J. and Fussell, J. C.: Size, source and chemical composition as determinants of toxicity

761 attributable to ambient particulate matter, *Atmos. Environ.*, 60, 504–526, 2012.

762

763 Keuken, M. P., Moerman, M., Zandveld, P., Henzing, J. S., and Hoek, G.: Total and size-resolved

764 particle number and black carbon concentrations in urban areas near Schiphol airport (the

765 Netherlands), *Atmos. Environ.*, 104, 132–142, 2015.

766

767 Kirkby, J. et al.: Role of sulphuric acid, ammonia and galactic cosmic rays in atmospheric aerosol

768 nucleation, *Nature*, 476(7361), pp. 429–435, 2011.

769

770 Kirkby, J., Curtius, J., Almeida, J., Dunne, E., Duplissy, J., Ehrhart, S., Franchin, A., Gagne, S., Ickes,

771 L., Kurten, A., Kupc, Metzger, A., Riccobono, F., Rondo, L., Schobesberger, S., Tsagkogeorgas, G.,

772 Wimmer, D., Amorim, A. A., Bianchi, F., Breitenlechner, M., David, A., Dommen, J., Downard, A.,

773 Ehn, M., Flagan, R. C., Haider, S., Hansel, A., Hauser, D., Jud, W., Junninen, H., Kreiss, F., Kvashin,

774 A., Laaksonen, A., Lehtipalo, K., Lima, J., Lovejoy, E. R., Makhmutov, V., Mathot, S., Mikkila, J.,

775 Minginette, P., Mogo, S., Nieminen, T., Onnela, A., Pereira, P., Petaja, T., Schnitzhofer, R., Seinfeld,

776 J. H., Sipila, M., Stozhkov, Y., Stratmann, F., Tome, A., Vanhanen, J., Viisanen, Y., Vrtala, A.,

777 Wagner, P. E., Walther, H., Weingartner, E., Wex, H., Winkler, P. M., Carslaw, K. S., Worsnop, D.

778 R., Baltensperger, U., and Kulmala M.: Ion-induced nucleation of pure biogenic particles, *Nature*.

779 Nature Publishing Group, 533, 521–526, 2016.

780

781 Korhonen, P., Kulmala, M., Laaksonen, A., Viisanen, Y., Mcgraw, R., and Seinfeld, J. H.: Ternary

782 nucleation of H_2SO_4 , NH_3 and H_2O in the atmosphere, *J. Geophys. Res.*, 104, D21, 26,349–26,353,

783 1999.

784

785 Kuang, C., McMurry, P. H., McCormick, A. V., and Eisele, F. L.: Dependence of nucleation rates on

786 sulfuric acid vapor concentration in diverse atmospheric locations, *J. Geophys. Res., Atmospheres*,

787 113, D10209, doi:10.1029/2007JD009253, 2008.

788

789 Kulmala, M., Dal Maso, M., Mäkelä, J. M., Pirjola, L., Väkevä, M., Aalto, P., Miikkulainen, P.,

790 Hämeri, K., and O’Dowd, C. D.: On the formation, growth and composition of nucleation mode

791 particles, *Tellus, Series B: Chem. Phys.Meteorol.*, 53, 479–490, 2001.

792

793 Kulmala, M., Kerminen, V.-M., Petäjä, T., Ding, A. J., and Wang, L.: Atmospheric gas-to-particle

794 conversion: why NPF events are observed in megacities?, *Faraday Discuss.*, 271–288, 2017.

795

796 Kulmala, M., Kontkanen, J., Junninen, H., Lehtipalo, K., Manninen, H. E., Nieminen, T., Petaja, T.,

797 Sipila, M., Schobesberger, S., Rantala, P., Franchin, A., Jokinen, T., Jarvinen, E., Aijala, M.,

798 Kangasluoma, J., Hakala, J., Aalto, P. P., Paasonen, P., Mikkilä, J., Vanhanen, J., Aalto, J., Hakola,
799 H., Makkonen, U., Ruuskanen, T., Mauldin, R. L., Duplissy, J., Vehkamäki, H., Back, J., Kortelainen,
800 A., Riipinen, I., Kurten, T., Johnston, M. V., Smith, J. N., Ehn, M., Mentel, T. F., Lehtinen, K. E. J.,
801 Laaksonen, A., Kerminen, V.-M., and Worsnop, D. R.: Direct Observations of Atmospheric Aerosol
802 Nucleation, *Science*, 339, 943–946, 2013.

803

804 Kulmala, M., Luoma, K., Virkkula, A., Petäjä, T., Paasonen, P., Kerminen, V. M., Nie, W., Qi, X.,
805 Shen, Y., Chi, X., and Ding, A.: On the mode-segregated aerosol particle number concentration load:
806 Contributions of primary and secondary particles in Hyytiälä and Nanjing, *Boreal Environ. Res.*, 21,
807 319–331, 2016.

808

809 Kulmala, M., Petäjä, T., Ehn, M., Thornton, J., Sipilä, M., Worsnop, D. R., and Kerminen, V.-M.:
810 Chemistry of Atmospheric Nucleation: On the Recent Advances on Precursor Characterization and
811 Atmospheric Cluster Composition in Connection with Atmospheric New Particle Formation,
812 *Ann.Rev.Phys. Chem.*, 65, 21–37, 2014.

813

814 Kulmala, M., Petäjä, T., Mönkkönen, P., Koponen, I. K., Dal Maso, M., Aalto, P. P., Lehtinen, K. E.
815 J., and Kerminen, V.-M.: On the growth of nucleation mode particles: source rates of condensable
816 vapor in polluted and clean environments, *Atmos. Chem. Phys. Discuss.*, 4, 6943–6966, 2005.

817

818 Kulmala, M., Petäjä, T., Nieminen, T., Sipilä, M., Manninen, H. E., Lehtipalo, K., Dal Maso, M.,
819 Aalto, P. P., Junninen, H., Paasonen, P., Riipinen, I., Lehtinen, K. E. J., Laaksonen, A., and Kerminen,
820 V. M.: Measurement of the nucleation of atmospheric aerosol particles, *Nature Protocols*, 7, 1651–
821 1667, 2012.

822

823 Kulmala, M., Vehkamäki, H., Petäjä, T., Dal Maso, M., Lauri, A., Kerminen, V. M., Birmili, W., and
824 McMurry, P. H.: Formation and growth rates of ultrafine atmospheric particles: A review of
825 observations, *J. Aerosol Sci.*, 35, 143–176, 2004.

826

827 Laaksonen, A., Kulmala, M., O’Dowd, C. D., Joutsensaari, J., Vaattovaara, P., Mikkonen, S.,
828 Lehtinen, K. E. J., Sogacheva, L., Dal Maso, M., Aalto, P., Petäjä, T., Sogachev, A., Yoon, Y. J.,
829 Lihavainen, H., Nilsson, D., Facchini, M. C., Cavalli, F., Fuzzi, S., Hoffmann, T., Arnold, F., Hanke,
830 M., Sellegri, K., Umann, B., Junkermann, W., Coe, H., Allan, J. D., Alfarra, M. R., Worsnop, D. R.,
831 Riekkola, M. L., Hyötyläinen, T., and Viisanen, Y.: The role of VOC oxidation products in
832 continental new particle formation, *Atmos. Chem. Phys.*, 8, 657–2665, 2008.

833

834 Ma, N. and Birmili, W.: Estimating the contribution of photochemical particle formation to ultrafine
835 particle number averages in an urban atmosphere, *Sci. Tot. Environ.*, 512–513, 154–166, 2015.

836

837

838 MacNee, W. and Donaldson, K.: Mechanism of lung injury caused by PM10 and ultrafine particles
839 with special reference to COPD, *Europ. Respirat. J.*, 21, 47S–51S, 2003.

840

841 Makkonen, R., Asmi, A., Kerminen, V. M., Boy, M., Arneth, A., Hari, P., and Kulmala, M.: Air
842 pollution control and decreasing new particle formation lead to strong climate warming, *Atmos.*
843 *Chem. Phys.*, 12, 1515–1524, 2012.

844

845 Masiol, M., Harrison, R. M., Vu, T. V., and Beddows, D. C. S.: Sources of sub-micrometre particles
846 near a major international airport, *Atmos. Chem. Phys.*, 17, 12379–12403, 2017.

847

848 Merikanto, J., Spracklen, D. V., Mann, G. W., Pickering, S. J., and Carslaw, K. S.: Impact of
849 nucleation on global CCN, *Atmos. Chem. Phys.*, 9, 8601–8616, 2009.

850

851 Metzger, A., Verheggen, B., Dommen, J., Duplissy, J., Prevot, A. S. H., Weingartner, E., Riipinen,
852 I., Kulmala, M., Spracklen, D. V., Carslaw, K. S., and Baltensperger, U.: Evidence for the role of
853 organics in aerosol particle formation under atmospheric conditions, *Proc. Natl. Acad. Sci.*, 107,
854 6646–6651, 2010.

855

856 Minguillón, M. C., Brines, M., Pérez, N., Reche, C., Pandolfi, M., Fonseca, A. S., Amato, F.,
857 Alastuey, A., Lyasota, A., Codina, B., Lee, H. K., Eun, H. R., Ahn, K. H., and Querol, X.: New
858 particle formation at ground level and in the vertical column over the Barcelona area, *Atmos. Res.*,
859 164–165, 118–130, 2015.

860

861 Napari, I., Noppel, M., Vehkamäki, H., and Kulmala, M.: An improved model for ternary nucleation
862 of sulfuric acid-ammonia-water, *J. Chem. Phys.*, 116, 4221–4227, 2002.

863

864 Németh, Z., Rosati, B., Zíková, N., Salma, I., Bozó, L., Dameto de España, C., Schwarz, J., Ždímal,
865 V., and Wonaschütz, A.: Comparison of atmospheric new particle formation events in three Central
866 European cities, *Atmos. Environ.*, 178, 191–197, 2018.

867

868 Németh, Z. and Salma, I.: Spatial extension of nucleating air masses in the Carpathian Basin, *Atmos.*
869 *Chem. Phys.*, 14, 8841–8848, 2014.

870

871 Nieminen, T., Kerminen, V.-M., Petäjä, T., Aalto, P. P., Arshinov, M., Asmi, E., Baltensperger, U.,
872 Beddows, D. C. S., Beukes, J. P., Collins, D., Ding, A., Harrison, R. M., Henzing, B., Hooda, R., Hu,
873 M., Hörrak, U., Kivekäs, N., Komsaare, K., Krejci, R., Kristensson, A., Laakso, L., Laaksonen, A.,
874 Leaitch, W. R., Lihavainen, H., Mihalopoulos, N., Németh, Z., Nie, W., O ’dowd, C., Salma, I.,
875 Sellegri, K., Svenningsson, B., Swietlicki, E., Tunved, P., Ulevicius, V., Vakkari, V., Vana, M.,
876 Wiedensohler, A., Wu, Z., Virtanen, A., and Kulmala, M.: Global analysis of continental boundary
877 layer new particle formation based on long-term measurements, *Atmos. Chem. Phys. Discuss*, 5194,

878 2018–304, 2018.

879

880 Nilsson, E. D., Paatero, J. and Boy, M.: Effects of air masses and synoptic weather on aerosol
881 formation in the continental boundary layer, *Tellus, Series B: Chem. Phys. Meteorol.*, 53, 462–478,
882 2001.

883

884 O’Dowd, C. D., Aalto, P., Hmeri, K., Kulmala, M., and Hoffmann, T.: Atmospheric particels from
885 organic vapours, *Nature*, 416, 497–498, 2002.

886

887 O’Dowd, C., Jimenez, J. L., Bahreini, R., Flagan, R. C., Seinfeld, J. H., Hameri Kaarle, Pirjola, L.,
888 Kulmala, M., Gerard Jennings, S., and Hoffmann, T.: Marine aerosol formation from biogenic iodine
889 emissions, *Nature*, 417, 1–5, 2002.

890

891 Oberdurst, G.: Toxicology of ultrafine particles: in vivo studies, *Philos. Trans. A. Math. Phys. Eng.*
892 *Sci.*, 358, 2719–2740, 2000.

893

894 Park, M., Yum, S. S., and Kim, J. H.: Characteristics of submicron aerosol number size distribution
895 and new particle formation events measured in Seoul, Korea, during 2004–2012, *Asia-Pacific J.*
896 *Atmos. Sci.*, 51, 1–10, 2015.

897

898 Peng, Y., Dong, Y., Li, X., Liu, X., Dai, J., Chen, C., Dong, Z., Du, C., and Wang, Z.: Different
899 Characteristics of New Particle Formation Events at Two Suburban Sites in Northern China,
900 *Atmosphere*, 8, 58, 2017.

901

902 Penttinen, P., Timonen, K. L., Tiittanen, P., Mirme, A., Ruuskanen, J., and Pekkanen, J.: Number
903 concentration and size of particles in urban air: Effects on spirometric lung function in adult asthmatic
904 subjects, *Environ. Health Perspect.*, 109, 319–323, 2001.

905

906 Petäjä, T., Mauldin, R. L., III, Kosciuch, E., McGrath, J., Nieminen, T., Paasonen, P., Boy, M.,
907 Adamov, A., Kotiaho, T., and Kulmala, M.: Sulfuric acid and OH concentrations in a boreal forest
908 site, *Atmos. Chem. Phys.*, 9, 7435–7448, 2009.

909

910 Pikridas, M., Sciare, J., Freutel, F., Crumeyrolle, S., Von Der Weiden-Reinmüller, S. L., Borbon, A.,
911 Schwarzenboeck, A., Merkel, M., Crippa, M., Kostenidou, E., Psichoudaki, M., Hildebrandt, L.,
912 Engelhart, G. J., Petäjä, T., Prévôt, A. S. H., Drewnick, F., Baltensperger, U., Wiedensohler, A.,
913 Kulmala, M., Beekmann, M., and Pandis, S. N.: In situ formation and spatial variability of particle
914 number concentration in a European megacity, *Atmos. Chem. Phys.*, 15, 0219–10237, 2015.

915

916 Politis, M., Pilinis, C., and Lekkas, T. D.: Ultrafine particles (UFP) and health effects. Dangerous.
917 Like no other PM? Review and analysis, *Global Nest J.*, 10, 439–452, 2008.

918 Rahman, M. M., Mazaheri, M., Clifford, S., and Morawska, L.: Estimate of main local sources to
 919 ambient ultrafine particle number concentrations in an urban area, *Atmos. Res.*, 194, 178–189, 2017.
 920
 921 Riccobono, F., Schobesberger, S., Scott, C. E., Dommen, J., Ortega, I. K., Rondo, L., Almeida, J.,
 922 Amorim, A., Bianchi, F., Breitenlechner, M., David, A., Downard, A., Dunne, E. M., Duplissy, J.,
 923 Ehrhart, S., Flagan, R. C., Franchin, A., Hansel, A., Junninen, H., Kajos, M., Keskinen, H., Kupc, A.,
 924 Makhmutov, V., Mathot, S., Nieminen, T., Onnela, A., Petäjä, T., Tsagkogeorgas, G., Vaattovaara,
 925 P., Viisanen, Y., Vrtala, A., and Wagner, P. E.: Oxidation Products of Biogenic Atmospheric
 926 Particles, *Science*, 717, 17–722, 2014.
 927
 928 Riipinen, I., Sihto, S.-L., Kulmala, M., Arnold, F., Dal Maso, M., Birmili, W., Saarnio, K., Teinilä,
 929 K., Kerminen, V.-M., Laaksonen, A., and Lehtinen, K. E. J.: Connections between atmospheric
 930 sulphuric acid and new particle formation during QUEST III–IV campaigns in Heidelberg and
 931 Hyytiälä, *Atmos. Chem. Phys.*, 7, 1899–1914, 2007.
 932
 933 Robinson, A. L., Donahue, N. M., Shrivastava, M. K., Weitkamp, E. A., Sage, A. M., Grieshop, A.
 934 P., Lane, T. E., Pierce, J. R., and Pandis, S. N.: Rethinking Organic Aerosols :, *Science*, 315, 1259–
 935 1262, 2007.
 936
 937 Rönkkö, T., Kuuluvainen, H., Karjalainen, P., Keskinen, J., Hillamo, R., Niemi, J. V., Pirjola, L.,
 938 Timonen, H. J., Saarikoski, S., Saukko, E., Järvinen, A., Silvennoinen, H., Rostedt, A., Olin, M., Yli-
 939 Ojanperä, J., Nousiainen, P., Kousa, A. and Dal Maso, M.: Traffic is a major source of atmospheric
 940 nanocluster aerosol, *Proc. Natl. Acad. Sci.*, 114, 7549–7554, 2017.
 941
 942 Salma, I., Borsós, T., Németh, Z., Weidinger, T., Aalto, P., and Kulmala, M.: Comparative study of
 943 ultrafine atmospheric aerosol within a city, *Atmos. Environ.*, 92, 154–161, 2014.
 944
 945 Salma, I., Németh, Z., Kerminen, V. M., Aalto, P., Nieminen, T., Weidinger, T., Molnár, Á., Imre,
 946 K., and Kulmala, M.: Regional effect on urban atmospheric nucleation, *Atmos. Chem. Phys.*, 16,
 947 8715–8728, 2016.
 948
 949 Salma, I., Varga, V., and Németh, Z.: Quantification of an atmospheric nucleation and growth process
 950 as a single source of aerosol particles in a city, *Atmos. Chem. Phys.*, 17, 15007–15017, 2017.
 951
 952 Samoli, E., Atkinson, R. W., Analitis, A., Fuller, G. W., Beddows, D., Green, D. C., Mudway, I. S.,
 953 Harrison, R. M., Anderson, H. R., and Kelly, F. J.: Differential health effects of short-term exposure
 954 to source-specific particles in London, U.K., *Environ. Intl.*, 97, 246–253, 2016.
 955
 956 Seinfeld, J. H. and Pandis, S. N.: *Atmospheric Chemistry and Physics: From Air Pollution to Climate*
 957 *Change*, 3rd Ed. New Jersey, Canada, John Wiley & Sons, Inc, 2012.

958 Shen, X., Sun, J., Kivekäs, N., Kristensson, A., Zhang, X., Zhang, Y., Zhang, L., Fan, R., Qi, X., Ma,
 959 Q. and Zhou, H.: Spatial distribution and occurrence probability of regional new particle formation
 960 events in eastern China, *Atmos. Chem. Phys.*, 185194, pp. 587–599, 2018.

961

962 Shi, J. P., Evans, D. E., Khan, A. A., and Harrison, R. M.: Sources and concentration of nanoparticles
 963 (<10nm diameter) in the urban atmosphere, *Atmos. Environ.*, 35, 1193–1202, 2001.

964

965 Shi, J. P. and Harrison, R. M.: Investigation of ultrafine particle formation during diesel exhaust
 966 dilution, *Environ. Sci. Technol.*, 33, 3730–3736, 1999.

967

968 Spracklen, D. V., Carslaw, K. S., Kulmala, M., Kerminen, V. M., Sihto, S. L., Riipinen, I., Merikanto,
 969 J., Mann, G. W., Chipperfield, M. P., Wiedensohler, A., Birmili, W., and Lihavainen, H.:
 970 Contribution of particle formation to global cloud condensation nuclei concentrations, *Geophys. Res.*
 971 *Lett.*, 35, 1–5, 2008.

972

973 Spracklen, D. V., Carslaw, K. S., Merikanto, J., Mann, G. W., Reddington, C. L., Pickering, S., Ogren,
 974 J. A., Andrews, E., Baltensperger, U., Weingartner, E., Boy, M., Kulmala, M., Laakso, L.,
 975 Lihavainen, H., Kivekäs, N., Komppula, M., Mihalopoulos, N., Kouvarakis, G., Jennings, S. G.,
 976 O’Dowd, C., Birmili, W., Wiedensohler, A., Weller, R., Gras, J., Laj, P., Sellegri, K., Bonn, B.,
 977 Krejci, R., Laaksonen, A., Hamed, A., Minikin, A., Harrison, R. M., Talbot, R., and Sun, J.:
 978 Explaining global surface aerosol number concentrations in terms of primary emissions and particle
 979 formation, *Atmos. Chem. Phys.*, 10, 4775–4793, 2010.

980

981 Sutton, M. A., Place, C. J., Eager, M., Fowler, D., and Smith, R. I.: Assessment of the magnitude of
 982 ammonia emissions in the UK, *Atmos. Environ.*, 29, 1393–1411, 1995.

983

984 Tröstl, J., Chuang, W. K., Gordon, H., Heinritzi, M., Yan, C., Molteni, U., Ahlm, L., Frege, C.,
 985 Bianchi, F., Wagner, R., Simon, M., Lehtipalo, K., Williamson, C., Craven, J. S., Duplissy, J.,
 986 Adamov, A., Almeida, J., Bernhammer, A.-K., Breitenlechner, M., Brilke, S., Dias, A., Ehrhart, S.,
 987 Flagan, R. C., Franchin, A., Fuchs, C., Guida, R., Gysel, M., Hansel, A., Hoyle, C. R., Jokinen, T.,
 988 Junninen, H., Kangasluoma, J., Keskinen, H., Kim, J., Krapf, M., Kürten, A., Laaksonen, A.,
 989 Lawler, M., Leiminger, M., Mathot, S., Möhler, O., Nieminen, T., Onnela, A., Petäjä, T., Piel, F. M.,
 990 Miettinen, P., Rissanen, M. P., Rondo, L., Sarnela, N., Schobesberger, S., Sengupta, K., Sipilä, M.,
 991 Smith, J. N., Steiner, G., Tomè, A., Virtanen, A., Wagner, A. C., Weingartner, E., Wimmer, D.,
 992 Winkler, P. M., Ye, P., Carslaw, K. S., Curtius, J., Dommen, J., Kirkby, J., Kulmala, M., Riipinen,
 993 I., Worsnop, D. R., Donahue, N. M., and Baltensperger, U.: The role of low-volatility organic
 994 compounds in initial particle growth in the atmosphere, *Nature*, 533, 527–531, 2016.

995

996 Von Bismarck-Osten, C., Birmili, W., Ketznel, M., Massling, A., Petäjä, T., and Weber, S.:
 997 Characterization of parameters influencing the spatio-temporal variability of urban particle number

998 size distributions in four European cities, *Atmos. Environ.*, 77, 415–429, 2013.
999
1000 Wang, Z., Wu, Z., Yue, D., Shang, D., Guo, S., Sun, J., Ding, A., Wang, L., Jiang, J., Guo, H., Gao,
1001 J., Cheung, H. C., Morawska, L., Keywood, M., and Hu, M.: New particle formation in China: Current
1002 knowledge and further directions, *Sci. Tot. Environ.*, 258–266, 2017.
1003
1004 Wehner, B., Siebert, H., Stratmann, F., Tuch, T., Wiedensohler, A., Petäjä, T., Dal Maso, M., and
1005 Kulmala, M.: Horizontal homogeneity and vertical extent of new particle formation events, *Tellus,*
1006 *Series B: Chem. Phys. Meteorol.*, 59, 362–371, 2007.
1007
1008 Woo, K. S., Chen, D. R., Pui, D. Y. H., and McMurry, P. H.: Measurement of Atlanta aerosol size
1009 distributions: Observations of lutrafine particle events, *Aerosol Sci. Technol.*, 34, 5–87, 2001.
1010
1011 Xiao, S., Wang, M. Y., Yao, L., Kulmala, M., Zhou, B., Yang, X., Chen, J. M., Wang, D. F., Fu, Q.
1012 Y., Worsnop, D. R., and Wang, L.: Strong atmospheric new particle formation in winter in urban
1013 Shanghai, China, *Atmos. Chem. Phys.*, 15, 1769–1781, 2015.
1014
1015 Yli-Juuti, T., Nieminen, T., Hirsikko, A., Aalto, P. P., Asmi, E., Hörrak, U., Manninen, H. E.,
1016 Patokoski, J., Dal Maso, M., Petäjä, T., Rinne, J., Kulmala, M., and Riipinen, I.: Growth rates of
1017 nucleation mode particles in Hyytiälä during 2003-2009: Variation with particle size, season, data
1018 analysis method and ambient conditions, *Atmos. Chem. Phys.*, 11, 12865–12886, 2011.
1019
1020 Yue, D. L., Hu, M., Zhang, R. Y., Wang, Z. B., Zheng, J., Wu, Z. J., Wiedensohler, A., He, L. Y.,
1021 Huang, X. F., and Zhu, T.: The roles of sulfuric acid in new particle formation and growth in the
1022 mega-city of Beijing, *Atmos. Chem. Phys.*, 10, 4953–4960, 2010.
1023
1024 Zhang, X., Zhang, Y., Sun, J., Zheng, X., Li, G., and Deng, Z.: Characterization of particle number
1025 size distribution and new particle formation in an urban environment in Lanzhou, China, *J. Aerosol*
1026 *Sci.*, 103, 53–66, 2017.
1027
1028
1029

1030 **TABLE LEGENDS:**

1031

1032 **Table 1:** Number of NPF events per site (in parenthesis the number of days with available
1033 data).

1034

1035 **Table 2:** Annual and seasonal NSF for all areas of study.

1036

1037

1038

1039 **FIGURE LEGENDS:**

1040

1041 **Figure 1:** Map of the measuring stations.

1042 **Figure 2:** Number of NPF events per season for all seven years of the present study (Winter –
1043 DJF; Spring – MAM; Summer – JJA; Autumn – SON) at Harwell (rural), N.
1044 Kensington (urban background) and Marylebone Road (urban roadside).

1045

1046 **Figure 3:** Growth rate per season at the three sites.

1047

1048 **Figure 4:** Diurnal variation of $N_{16-20nm}$ at each site: annual mean and NPF event days.

1049

1050 **Figure 5:** Map and frequency of incoming air mass origin – average and for NPF events per site.

1051

1052 **Figure 6:** Growth rate per incoming air mass at each of the sites.

1053

1054 **Figure 7:** Survival parameter P (a) per season, (b) for regional and local events (for Marylebone
1055 Road) is regional for all 3 sites and (c) by incoming air mass origin.

1056

1057

1058 **Table 1:** Number of NPF events per site (in parenthesis the number of days with available data).
1059

	Harwell	N. Kensington	Marylebone Road	Regional (Background sites)*	Regional (All 3 sites)**
2009	9 (210)	0 (332)	4 (290)	0	0
2010	29 (262)	22 (310)	22 (292)	11	9
2011	15 (291)	10 (300)	23 (284)	4	1
2012	8 (334)	28 (303)	12 (140)	3	0
2013	25 (328)	23 (342)	27 (334)	13	11
2014	29 (324)	34 (330)	13 (314)	18	6
2015	25 (282)	22 (314)	18 (338)	11	10
Overall	140 (2031)	139 (2231)	119 (1993)	60	37

1060 * Refers to events occurring simultaneously at Harwell and N. Kensington

1061 ** Refers to events which occur simultaneously at all three sites

1062
1063
1064

1065 **Table 2:** Annual and seasonal NSF for all areas of study.
1066

	Harwell	N. Kensington	Marylebone Road
NSF _{NUC} (Spring)	2.04±0.61	2.03±0.48	1.20±0.26
NSF _{NUC} (Summer)	2.01±0.94	1.72±0.57	1.26±0.34
NSF _{NUC} (Year)	2.25±0.85	1.86±0.56	1.26±0.31
NSF _{GEN} (Spring)	1.10±0.57	1.07±0.54	1.02±0.30
NSF _{GEN} (Summer)	1.18±0.79	1.11±0.61	1.01±0.23
NSF _{GEN} (Year)	1.10±0.61	1.06±0.54	1.02±0.27

1067



1068
1069

1070 **Figure 1:** Map of the measuring stations.

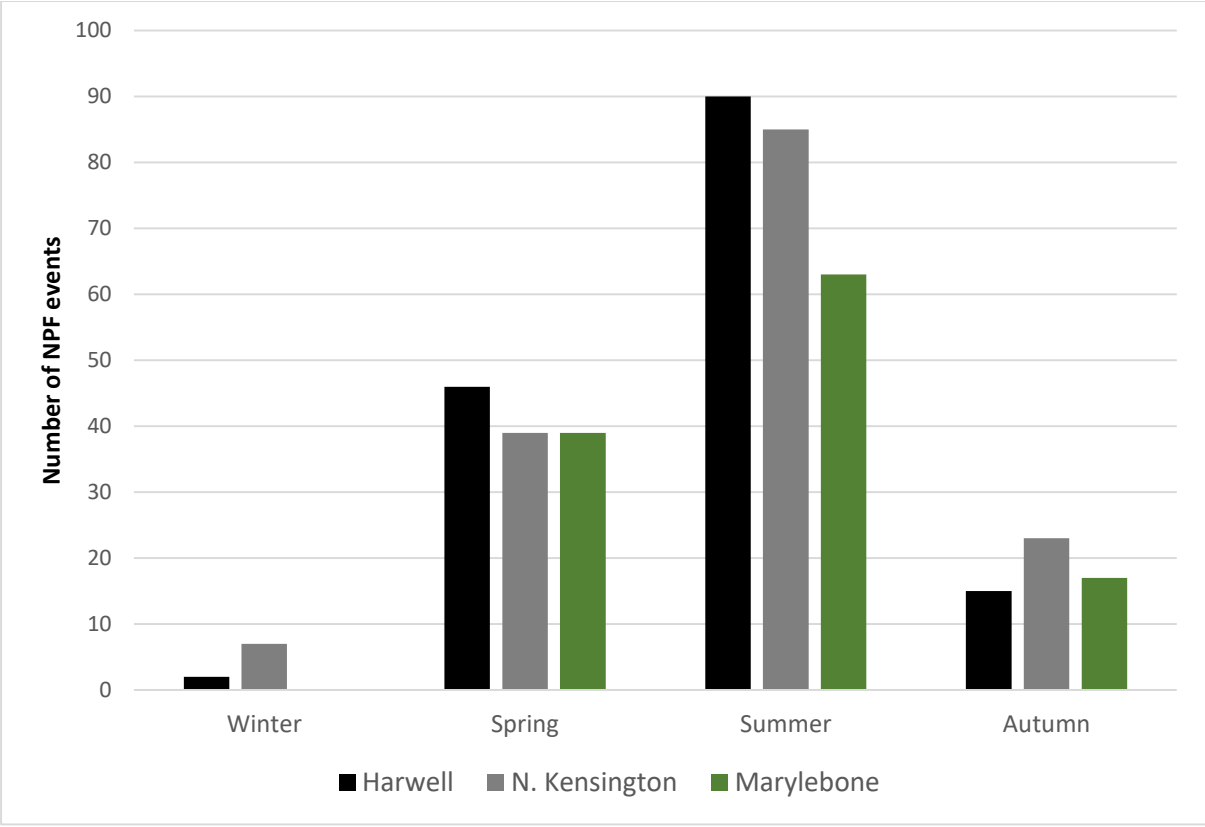


Figure 2: Number of NPF events per season for all seven years of the present study (Winter – DJF; Spring – MAM; Summer – JJA; Autumn – SON) at Harwell (rural), N.Kensington (urban background) and Marylebone Road (urban roadside).

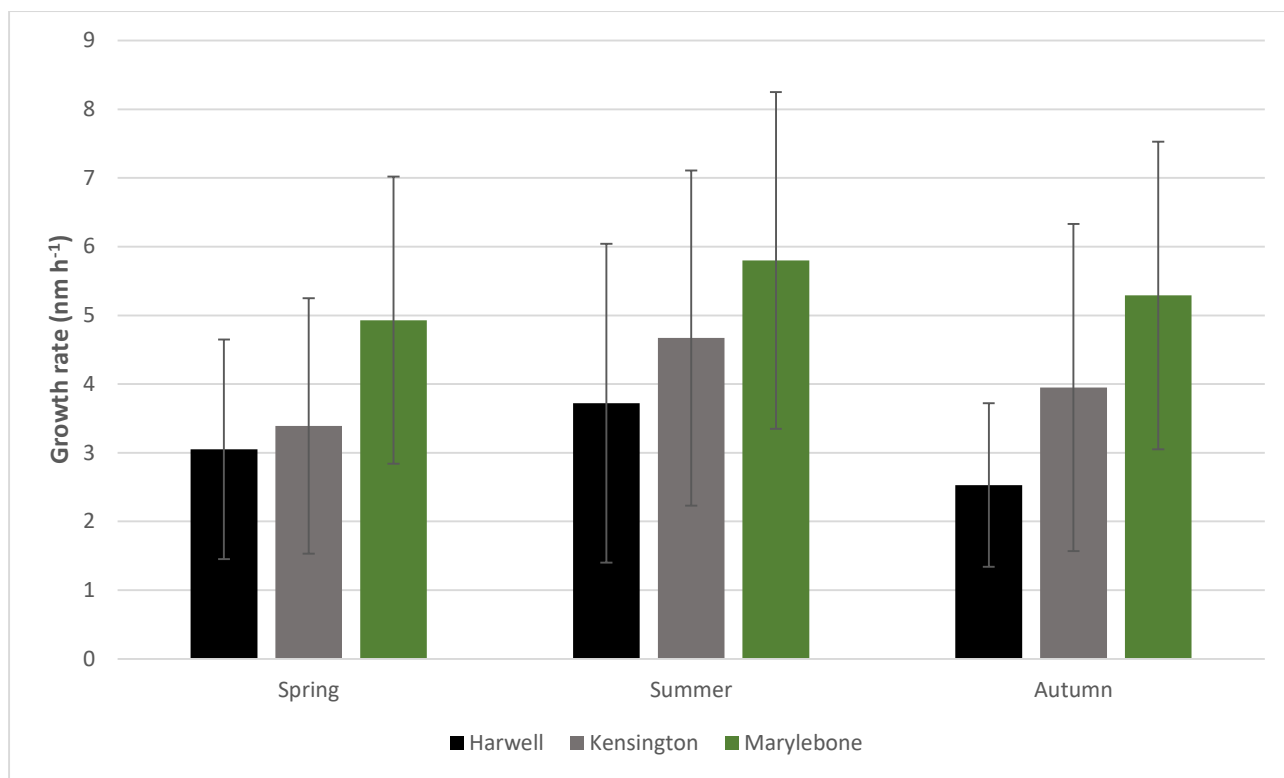
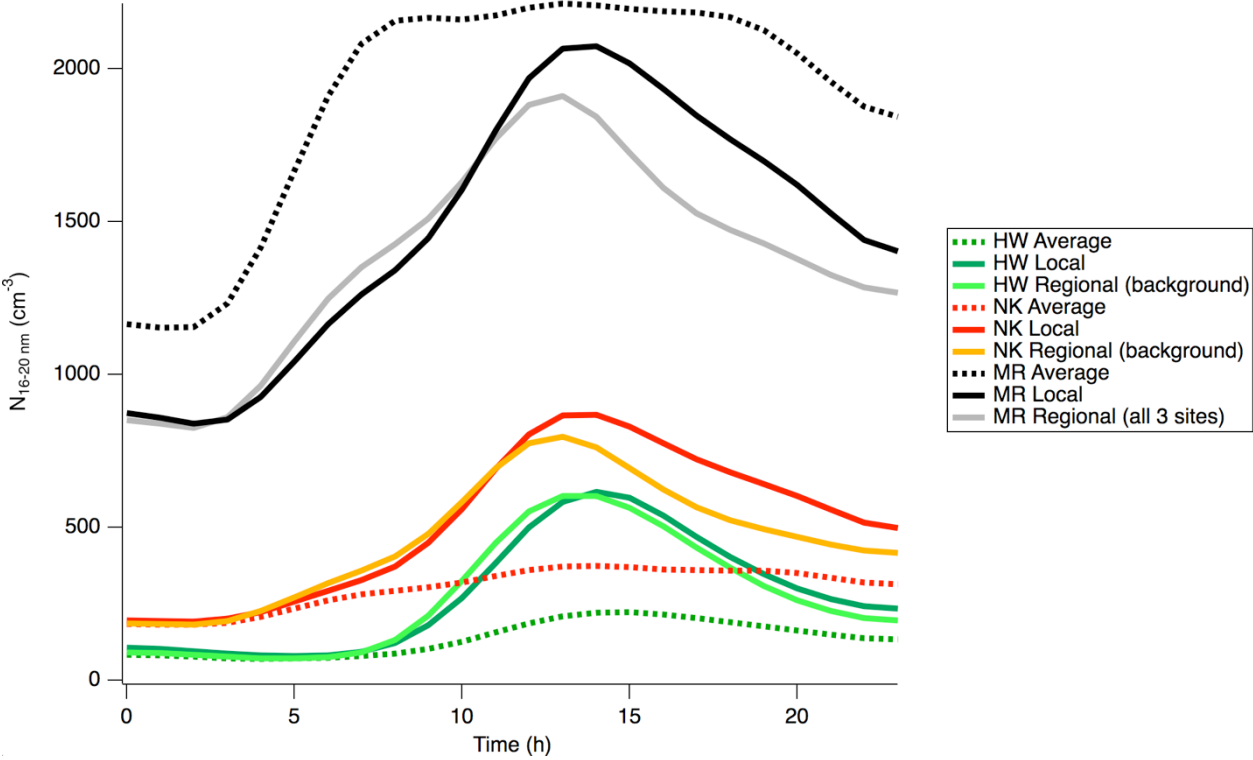


Figure 3: Growth rate per season at the three sites.

1097



1098

1099

1100

1101

1102

1103

1104

1105

1106

1107

1108

1109

1110

1111

1112

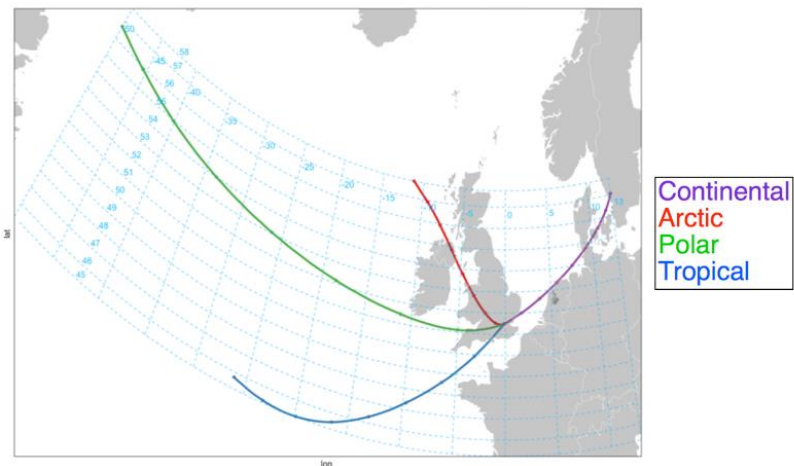
1113

1114

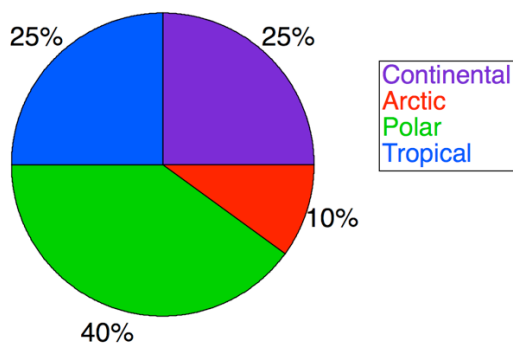
1115

1116

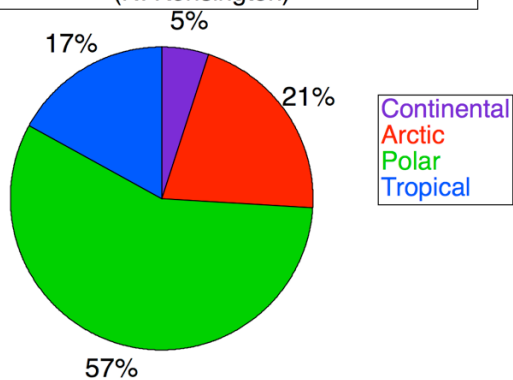
Figure 4: Diurnal variation of $N_{16-20\text{nm}}$ at each site: annual mean and NPF event days.



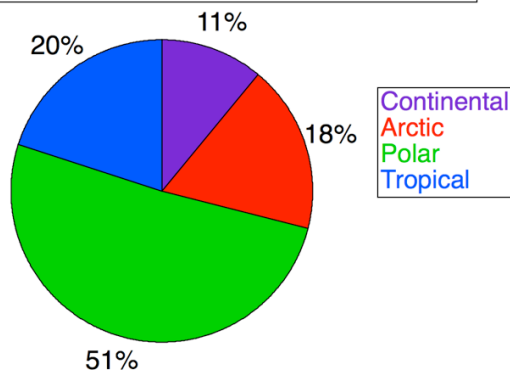
Frequency per air mass trajectory



Frequency of event days per air mass trajectory (N. Kensington)



Frequency of event days per air mass trajectory (Harwell)



Frequency of event days per air mass trajectory (Marylebone Road)

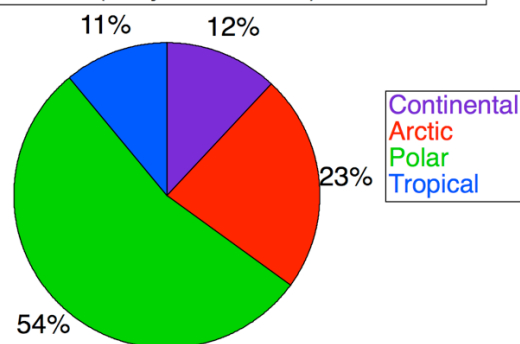


Figure 5: Map and frequency of incoming air mass origin – average and for NPF events per site.

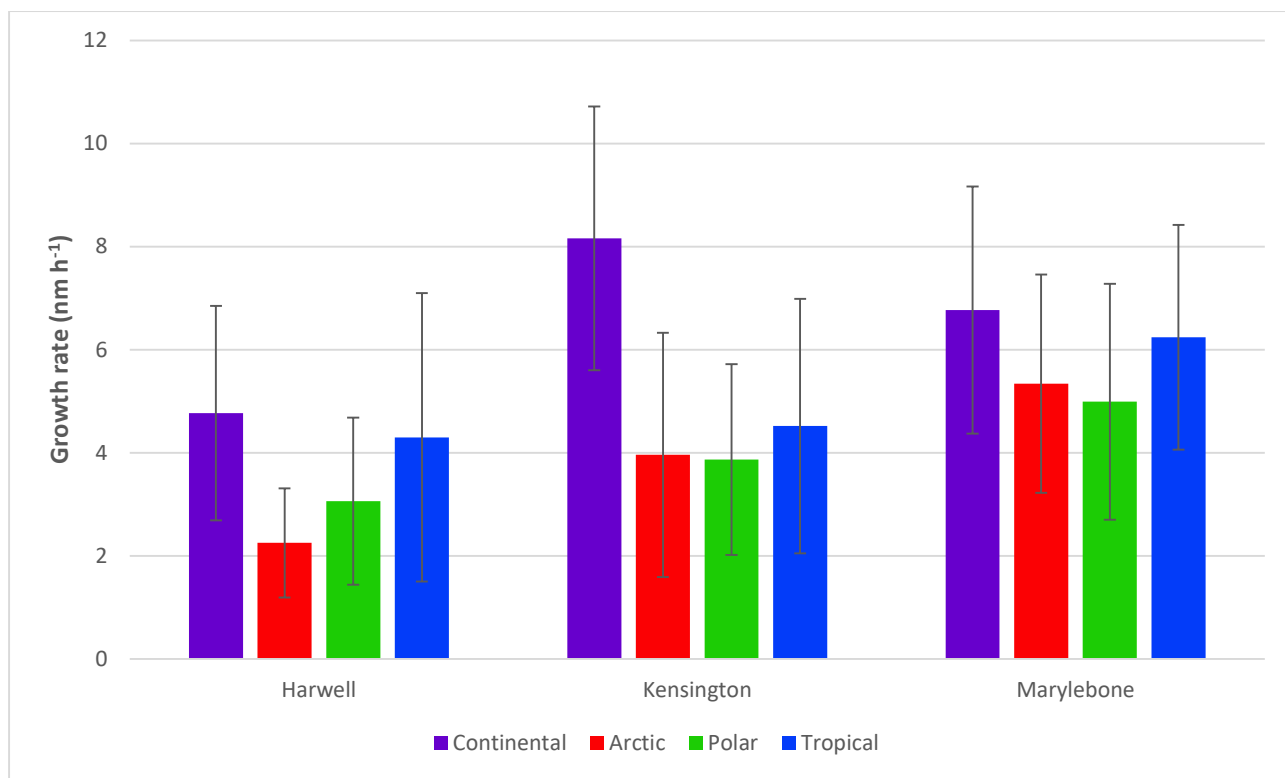
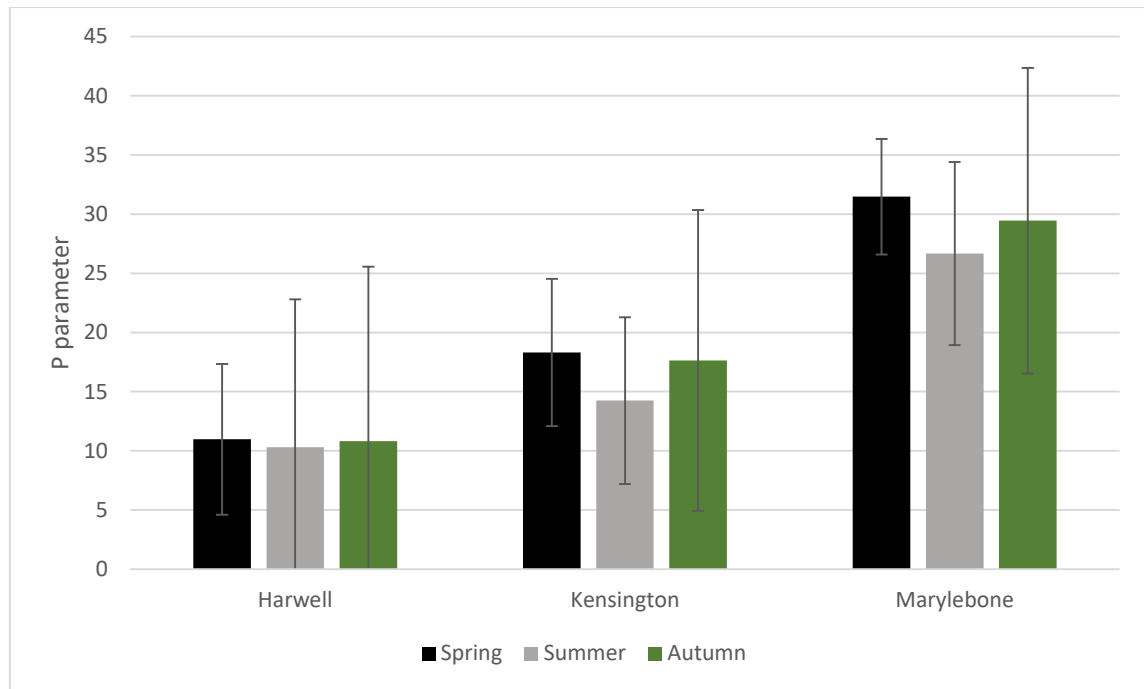


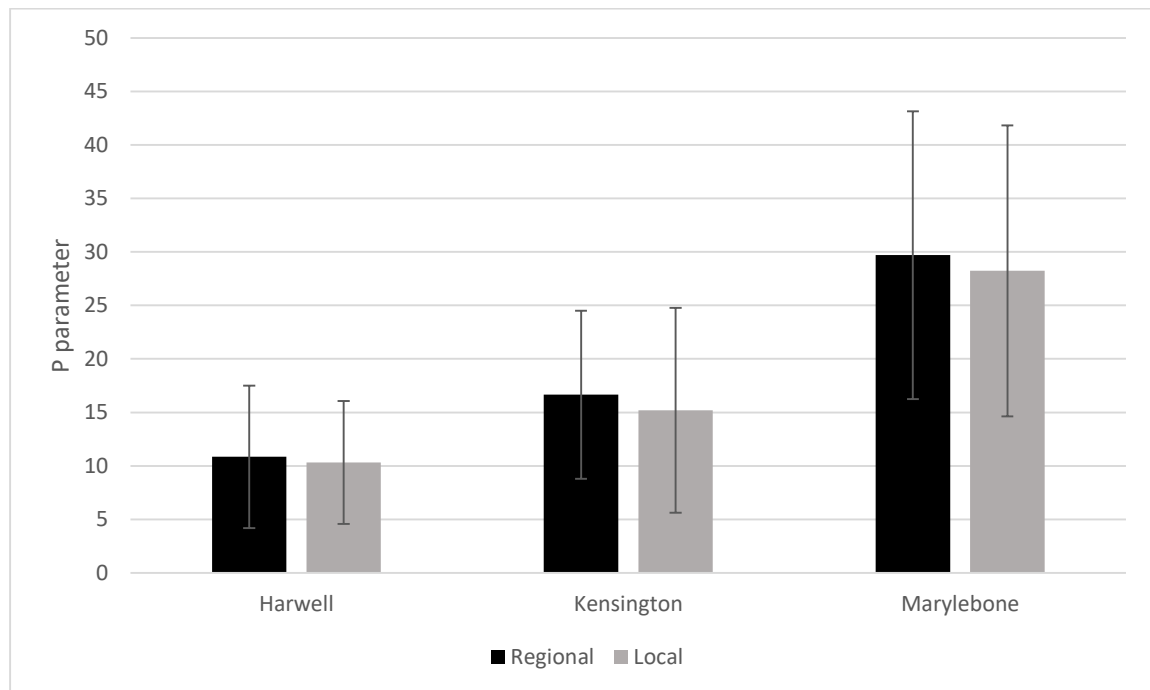
Figure 6: Growth rate per incoming air mass origin at each of the sites.

(a)



1130
1131

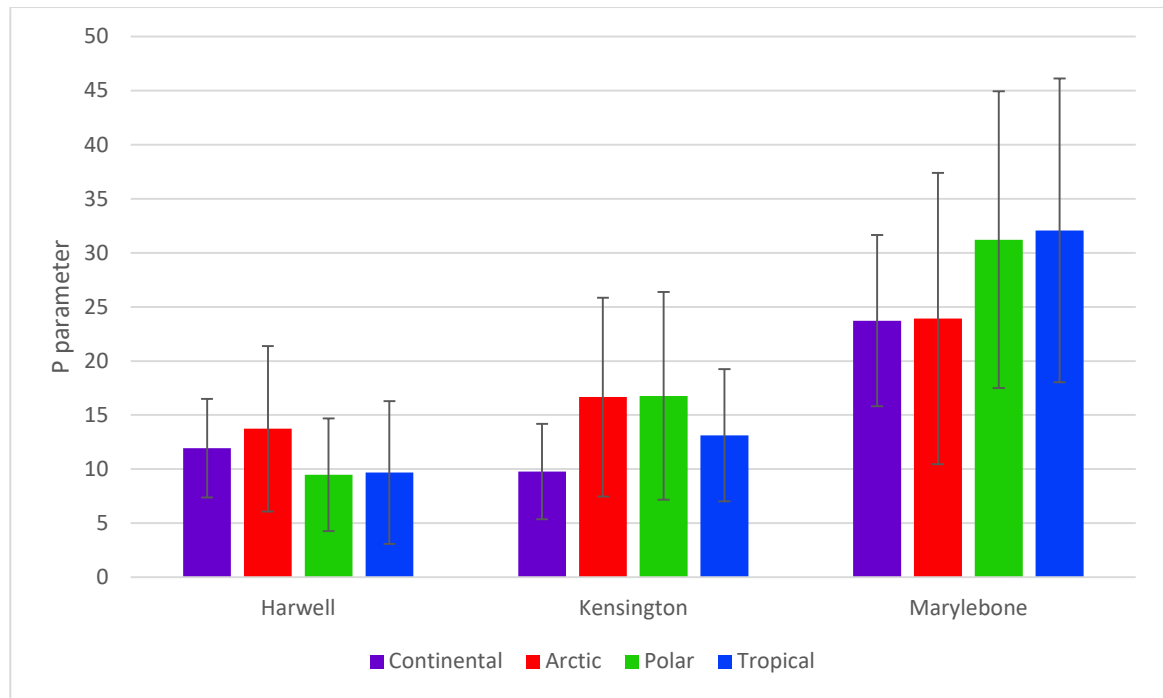
(b)



1132

1133
1134

(c)



1135

1136 **Figure 7:** Survival parameter P (a) per season, (b) for regional and local events (for Marylebone
1137 Road regional is for all 3 sites) and (c) by incoming air mass origin.

1138

1139

1140

1141